Africánes in southern Africa: attributes and contribution to rainfall of a continental tropical low.

Elizabeth Viljoen[1,2], Liesl Dyson[2] and Ishmael Moyo[1,2]

[1] South African Weather Service, Pretoria, South Africa

[2] Department of Geography, Geoinformatics and Meteorology, University of Pretoria, South Africa

Corresponding author: liesl.dyson@up.ac.za

Elizabeth Viljoen: https://orcid.org/0000-0003-2844-3295

Liesl Dyson: https://orcid.org/0000-0003-2931-8824

Ishmael Moyo: https://orcid.org/0000-0003-1970-2371

Abstract

Large parts of southern Africa are influenced by extra-tropical weather systems for most of the year. During late summer (December to March), the circulation over the area becomes distinctly tropical. This paper introduces the Africáne, a synoptic scale tropical low-pressure system which has been shown to cause widespread and heavy rainfall over the southern sub-continent of Africa. The frequency of occurrence of Africánes, their contribution to rainfall and interannual variability are discussed in this paper. Africánes occur most frequently at the longitude of the Caprivi area with a second peak in frequency at around 32.5˚E. They mostly occur over Namibia, Botswana and Zimbabwe and only infrequently infiltrate as far south as the borders of South Africa. However, when they do occur over South Africa, they cause widespread heavy rainfall and floods. Rainfall is mostly confined to the eastern flank of Africánes and between 20-35% of the annual rainfall over southern Africa in late summer can be attributed to these systems. There are two main synoptic regimes associated with Africánes: a westerly wave or tropical-temperature trough combines with the Africáne to pull rainfall southwards into South Africa. The second, is a mid-level subtropical high pressure, located south of the Africáne, which causes the rainfall to be confined to the north. The interannual variability of Africánes are closely linked to rainfall over southern Africa, such that an above normal number of Africánes in a season causes above normal rainfall over southern Africa. The number of Africánes that form per year is linked to El Niño–Southern Oscillation (ENSO). It is recommended that the predictability of Africánes on different time scales should be investigated.

Keywords: continental tropical low; heavy rainfall; southern Africa; tropical temperature trough; Angola low.

Declaration

Funding

The MSc study of Elizabeth Viljoen (nee Webster) was funded by the South African Water Research Commission

Conflicts of interest/Competing interests

Not applicable

Availability of data and material

All data used in the paper are public good data. All output data are available on request

Code availability

Available on request

Authors' contributions

Elizabeth Viljoen (née Webster) conducted a significant amount of the research as part of her MSc qualification

Liesl Dyson, supervised the MSc study, conducted part of the research and edited the manuscript.

Ishmael Moyo contributed to the general circulation and dynamics investigation as part of on-going research

1. Introduction

The tropical region can generally be defined as the area between the Tropic of Cancer (23.5°N) and the Tropic of Capricorn (23.5°S) (Asnani, 2005). Tropical weather systems, however, are not fixed by these boundaries, but rather follow the position of the sun.

The deep tropics (15˚N to 15˚S) (Seidel et al., 2001) are largely characterised by rising air (Laing and Evans, 2016) and the Hadley cell causes the transport of heat and momentum to higher latitudes (Asnani, 2005). The equatorial zone (10˚N to 10˚S) is dominated by the equatorial trough, with the subtropical high-pressure belt over the subtropics (Riehl, 1979). This paper focuses on the area between these two belts where easterly winds are prevalent.

The tropical region experiences a vast range of weather, from clear skies during the dry seasons to excessive rain and extreme winds that are often associated with tropical cyclones (Ramage, 1995). Tropical weather systems are known to cause devastation across the globe due to flooding, however, many parts of the world rely on the rainfall produced by these weather systems for potable water and to sustain agriculture and other economic activities (Anthes, 2016).

The focus of this paper is tropical low pressures that develop over land. In north Africa, African easterly waves (AEWs) develop during boreal summer in the lower troposphere, occur regularly (3-5-day periodicity) and are westward moving disturbances (Berry et al., 2007, Burpee, 1972, Gu et al., 2004). Approximately 60 AEWs occur on average over north Africa between May and October (AMS, 2022). AEWs play an important role in the climate and precipitation of north Africa and their occurrence are closely related to the march of the inter-tropical convergence zone (ITCZ) (Gu et al., 2004). Tropical low-pressure systems which develop or intensify overland have been observed in Australia. These lows are informally referred to as *landphoons* (May et al., 2008, Tang et al., 2016) and they are often responsible for extraordinary rainfall and flooding over wide areas. Hunt et al. (2016) provide detail on the structure and dynamics of monsoon depressions in India and describe how some of these lows track westwards along the southern edge of the Himalayas. Monsoon depressions and their weaker counterparts, monsoon lows, are responsible for widespread and heavy rainfall in India (Hunt and Fletcher, 2019). Hurley and Boos (2015) found that between 15 and 20 summer monsoon low-pressure systems occur over India while Berry et al. (2012) identified between 12 and 15 synoptic scale monsoon lows over Australia during Austral summer. Howard and Washington (2018) found that some of the characteristics of landphoons in Australia and monsoon depressions in India are comparable to tropical lows in southern Africa. Southern Africa (SA) is defined in this paper as continental Africa south of 15˚S (Fig. 1).

Tropical weather systems invade SA during the summer months (December to March) (Dyson and Van Heerden, 2002, Tyson and Preston-Whyte, 2000), which coincides with the rainfall peaks of this area (Richard et al., 2001). The frequency of tropical disturbances in SA between April and October is low (Tyson and Preston-Whyte, 2000). Taljaard (1996) identified four main tropical weather systems that affect SA weather; tropical cyclones (Chikoore et al., 2015, Malherbe et al., 2012); tropical temperate troughs (TTTs) (Hart et al., 2013); tropical low pressures (Dyson and Van Heerden, 2002, Howard and Washington, 2018) and the ITCZ.

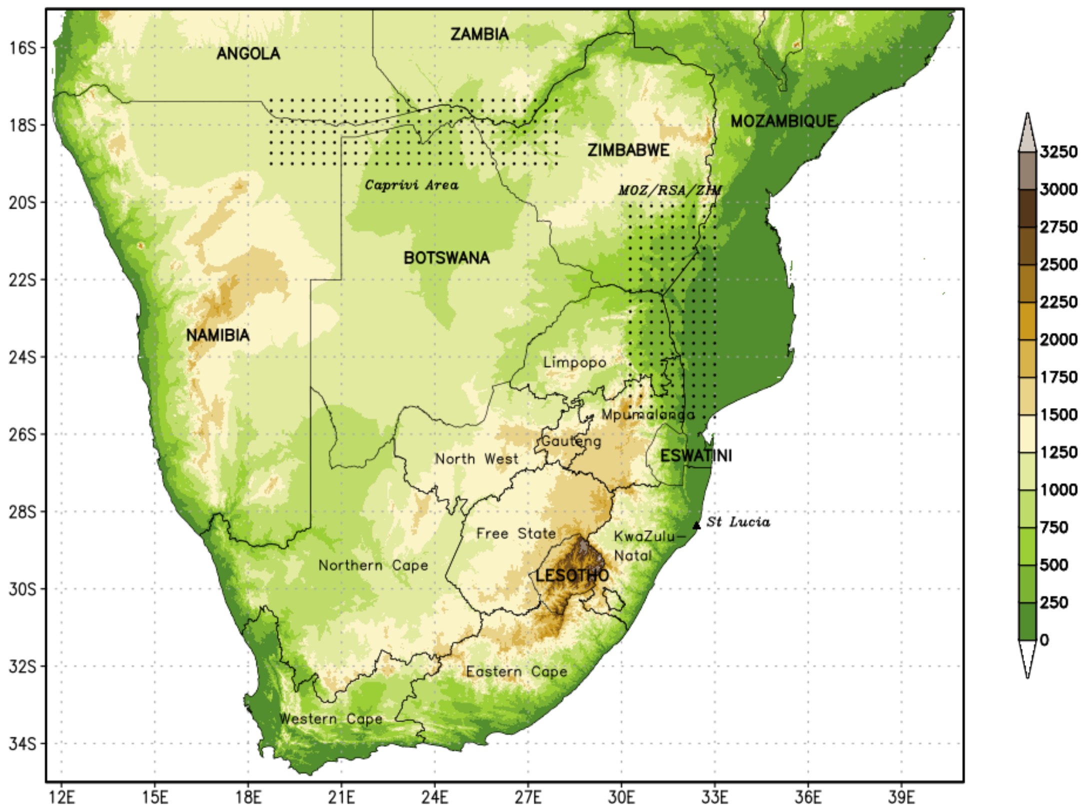

Figure 1: Topographical and location map of southern Africa. The dotted shades indicate the Caprivi area and the border between Mozambique, South Africa and Zimbabwe (MOZ/RSA/ZIM).

During late summer months, when the ITCZ extends as far south as 17˚ (Taljaard, 1995), a semi-stationary low-level tropical low develops over Angola (Taljaard, 1953), extending a trough southward into South Africa (Williams et al., 1984). This low pressure was first named the Angola low by Zunckel et al. (1996) and its characteristics investigated by Mulenga (1998). Reason et al. (2006) described the Angola low as a shallow heat low but Howard and Washington (2018) identified the Angola tropical low when the low becomes moist and deep. They identified the low as being associated with potential vorticity extending from the surface to about 300 hPa, and being cool near the surface but warm in the upper troposphere. The Angola low is recognised as a cyclonic, moisture convergence area and a governing feature of rainfall over SA (Mulenga, 1998). The forecast drought during the El Niño of 1997/1998 did not occur and Blamey et al. (2018) and Reason and Jagadheesha (2005) contribute this to an anomalously strong Angola low in that season. Howard et al. (2019) found that as much as 66% of the November-March rainfall in south-west Angola is from tropical lows.

In some instances, tropical lows will interact with temperate westerly troughs and form cloud bands across the subcontinent (Washington and Todd, 1999). These long bands of clouds, as seen on satellite imagery, are one of the major distinguishing features of the Southern Hemisphere circulation (Harrison, 1984), and are known as tropical-temperate troughs (TTTs). TTTs can be described as areas of increased convergence that connect tropical and temperate systems (Hart et al., 2013), and transport energy, moisture and momentum from the tropical to the temperate regions (Harrison, 1984, van den Heever et al., 1997). TTTs are not unique to southern Africa, but can be found in several regions, including Australia and South America (Hart et al., 2010, van den Heever et al., 1997, Hauser et al., 2020). Crimp (1997) and Hart et al. (2013) found that TTTs contribute approximately 30% of the total rainfall for October and December, 60% of the total rainfall for January and 39% of the mean annual total for SA. Rainfall mostly occurs in and east of a TTT as an eastward moving mid-level westerly (temperate) trough increases upper air divergence on its leading edge. This happens above an area where warm tropical air is advected southward over SA from the tropical low and therefore enhancing uplift and convective cloud development (Hart et al., 2010).

SA is an area where tropical and temperate weather systems co-exist and interact. Taljaard (1985) explained how confusion exists in distinguishing cut-off lows (COLs) from lows in the tropical easterlies. He also stated that tropical lows are warm cored in the middle and upper troposphere, and this results in a ridge near the tropopause, superimposed over the low closer to the surface. Taljaard’s (1985) findings are echoed by Triegaardt et al. (1991) who investigated the heavy rainfall producing synoptic scale tropical low that occurred over SA in February 1988. These authors described how convective (or potential) instability could be applied to identify tropical weather systems. These two authors (and others) described synoptic scale tropical weather systems which caused heavy rainfall over South Africa and how these lows were located a considerable distance away from Angola. The February 1988 low was situated as far south as the western Botswana/South Africa border, causing heavy rainfall over central South Africa (Triegaardt et al., 1991). Dyson and Van Heerden (2002) discussed a continental tropical low which occurred over south-eastern

Botswana in 2000 when heavy rainfall fell for four consecutive days over Gauteng, North-West and eastern Limpopo provinces (see Fig. 1 for locations) resulting in widespread flooding. Webster (2019) described a continental tropical low that developed over Zimbabwe in January 2013, moved westward to the Caprivi area (Fig. 1) and then returned to Zimbabwe and Mozambique where it eventually moved into the Mozambique Channel. Devastating floods occurred in eastern South Africa where 12 people died and a further 9 in Mozambique.

Considering the geographical position of continental tropical low-pressure systems which have been shown to cause heavy rainfall over South Africa, there is a need to define a tropical low of considerable strength which may develop and traverse over most of the southern sub-continent of Africa. This low may be considered a very specific subset of the Angola low. In the presented research we introduce *Africánes.* The name is inspired by the name *Medicane* given to tropical hurricane like systems which occur over the Mediterranean Sea (Cavicchia et al., 2014). The intention is not to equate Medicanes and Africánes as the two systems are different. Medicanes are mesoscale cyclones which occur over the Mediterranean Sea (Cavicchia et al., 2014), while Africánes are large synoptic scale lows which occur over the continent of Africa (Dyson and Van Heerden, 2002). Strict circulation and thermodynamic criteria are applied to objectively identify Africánes which present as weak tropical cyclones (see section 2 and 5). The main focus is to identify tropical lows which develop over the interior of the southern subcontinent of Africa. However, tropical cyclones making landfall over the eastern seaboard often weaken into lows over the continent that exhibit the same characteristics as Africánes. The paper aims to address the following questions: 1. What is the geographical distribution of Africánes over SA? 2. What proportion of rainfall in SA can be attributed to Africánes? 3. Does an association exist between the interannual variability of Africánes over SA and ENSO?

The objective method to identify Africánes is presented in section 2. The data and methodology used are described in section 3 and the geographical distribution of Africánes is discussed in section 4. Section 5 presents Africáne circulation dynamics while their contribution to rainfall over SA is shown in section 6. In section 7 the interannual variability of Africánes are demonstrated.

2. Objective Identification Method

Several objective methods to identify synoptic weather systems using Numerical Weather Predication data have been developed and/or applied over SA. COLs have received special attention as Engelbrecht et al. (2015); Favre et al. (2013) and Singleton and Reason (2007) all defined circulation criteria to identify COLs over SA. Engelbrecht et al. (2013) identified closed mid-tropospheric lows but did not distinguish between cold and warm lows. Tropical weather systems have also received some attention as Malherbe et al. (2012) developed a method to identify westward moving tropical lows over the Mozambique Channel and Howard et al. (2019) used a tracking algorithm (TRACK) to identify Angola lows over sub-tropical SA. The tracking algorithm is described by Hodges (1994).

The research presented in this paper builds on the work of Webster (2019) who constructed objective methods to identify continental tropical lows (CTLs) over SA. These methods are broadly based on work done by Dyson and Van Heerden (2002) who developed a Model for the Identification of Tropical weather Systems (MITS). MITS is a process where subjective methods are used to identify strong, heavy rainfall producing, tropical low-pressure systems over SA but which also sometimes occur inside the borders of South Africa. Stricter criteria than those developed by Howard et al. (2019) to identify the Angola low are needed to identify these tropical cyclone-like lows over SA.

The objective identification method requires four strict criteria to be met (Fig. 2). The first criterium is a Favourable Tropical Environment (FTE) (Webster, 2019) (1 on Fig. 2). The first essential feature of an FTE is to identify an upright low-pressure system which is replaced by a high close to the tropopause. The upright low is identified by isolating areas where negative relative vorticity values exist at 850 and 500 hPa, while the high is represented by positive relative vorticity values at 300 hPa. In order to guarantee that only strong tropical lows are identified, the upright low should be deeper and the high near the tropopause stronger than normal. This is done by stipulating that the deviation from the normal relative vorticity values for the month under investigation, show anomalously strong circulation. The other features of an FTE comprise of atmospheric variables which have been shown to identify the tropical nature of the atmosphere. An FTE should have above normal total static energy (TSE) values, average 500-300 hPa temperatures as well as precipitable water values. The last requirement for an FTE is that precipitable water from 850-300 hPa should be greater than 20 mm (Dyson and Van Heerden, 2002).

Once an FTE has been identified, it is required that a closed 500 hPa geopotential low with a warm core (500-300 hPa) exist within close proximity of the FTE (2 and 3 On Fig. 2). The low (warm core) is identified by comparing the geopotential height (temperature) value at every grid point, to the values at the surrounding grid points. A closed low (warm core) is noted when the geopotential height (temperature) value at any particular grid point is lower (higher) than the values at the surrounding grid points. The last criteria in identifying an Africáne is that the warm FTE low should exist for at least 18 hours (4 on Fig. 2).

Once a grid point meets all these criteria, the position of the closed 500 hPa low pressure is used as the location of the Africáne. Further fine tuning is needed to consider large Africánes that extend over more than one adjacent grid point at a particular time step. Under these circumstances the grid point closest to the average position of the Africáne is used as the location of the Africáne and therefore only one Africáne is counted at that time. This eliminates the possibility of one large Africáne being counted multiple times.

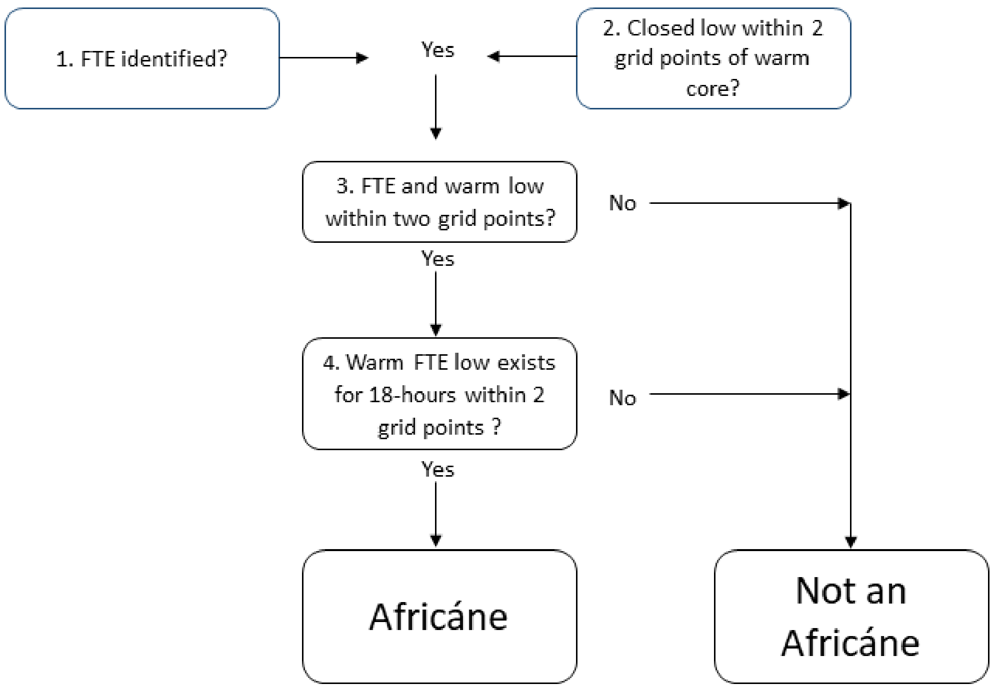

Figure 2: Flow diagram illustrating the procedure used to objectively identify Africánes over southern Africa.

3. Data and method

NCEP Reanalysis 2 data provided by the NOAA/OAR/ESRL PSL, Boulder, Colorado, USA, from their Website at https://psl.noaa.gov/data/gridded/data.ncep.reanalysis2.html was used to identify Africánes over December to March for each year between 1981 and 2020. Engelbrecht et al. (2013) stated that tropical low pressures have a horizontal scale of 500-1000 km and as the NCEP data set has a horizontal resolution of 2.5˚ (approximately 250 km), it makes it suitable to investigate synoptic scale weather systems (Engelbrecht et al., 2015, Favre et al., 2013, Malherbe et al., 2012, Singleton and Reason, 2007). A landmask is used at the end of the identification process in order to identify Africánes only over the continent of Africa.

In section 4, results are presented on the analysis performed at 6-hourly instantaneous intervals (temporal resolution of NCEP Reanalysis 2 data) and several Africánes may be identified on a day. An Africáne day is defined as a day on which an Africáne occurred at any time. Africáne days are used to investigate the proportion of rainfall contributed to Africánes in Section 6.

The Climate Hazards Group InfraRed Precipitation with Station data (CHIRPS) precipitation data set was used to do the rainfall analysis (Funk et al., 2015). The CHIRPS data set is a combination of rainfall estimates from satellite and station rainfall data.

4. Geographical and seasonal distribution of Africánes

Africánes were only identified to occur north of 27.5˚ S over SA (Fig. 3). In total there were 2190 Africánes at 6-hourly time steps with close to 90% identified at the grid points at 17.5˚S (64%) and 20˚S (24%). The highest frequency of incidence is in the Caprivi area (see Fig.1 for location) and more than 200 Africánes occurred per grid point in the 39-year period (between 5 and 7 per annum) over the central Caprivi area. This area is slightly south-east of where Howard et al. (2019) identified the highest frequency of Angola lows. The large number of Africánes identified in this area demonstrates the importance of tropical low development in the Caprivi area and surrounds to understanding the climate of SA. The number of Africánes decreased southwards, but at 20˚S there were still more than 50 Africánes (1.5 to 3 per annum) per grid point, except in the extreme west (Fig. 3). At 22.5˚ S, there are two areas where between 20 and 50 Africánes were identified. The first area over central Botswana and the Botswana/Namibia border, south of the high frequency Africáne zone over the Caprivi area, and the second area over Mozambique. Further south, less than 20 Africánes were identified per grid point with the lowest frequency over southern Namibia. Only 12% of the total number of Africánes were identified at the grid points 22.5˚S and 27.5˚S. However, as will be indicated in section 6, Africánes at these southern locations result in heavy rainfall over SA. Over the entire sub-continent, the lowest number of Africánes occurred in the west with a peak between 20 and 25˚E and a second, lower, peak at 32.5˚E.

Similar to the findings of Howard and Washington (2018), the highest number of Africánes were identified during January (801), followed by February (748) then December (337) with the lowest number in March (304) (Fig. 4). The monthly geographical distribution of Africánes mimics the distribution in Fig.3. with only slight differences. The highest number of Africánes were identified over the Caprivi area every month with the maximum number per latitude extending southwards from there. Africánes were identified to extend further south in February over the central interior, albeit with very low frequencies. The second eastern peak in Africáne occurrence is also present in the monthly maps and is most pronounced in January and February.

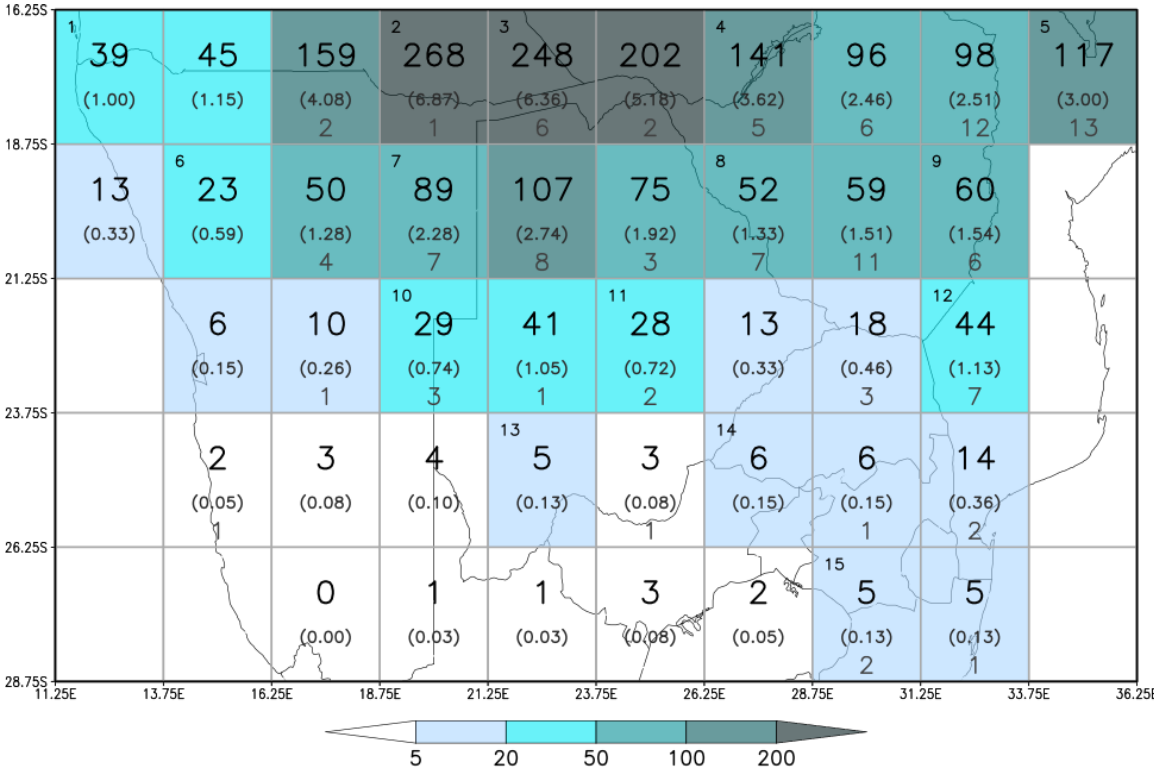

Figure 3: Total number of Africánes per 2.5˚ x 2.5˚ NCEP grid box for the 39 summer seasons (Dec-Mar) between 1981 and 2020 and the annual Africáne frequency (number in brackets). The total number of Africánes was calculated at 6-hourly time steps and more than one Africáne may be identified on a day. The total number of Africánes are indicated in the centre of each grid box. The number at the bottom of the grid box indicates the number of ex-tropical cyclone Africánes identified in the grid box. The number in the top left of the grid box is the location number of 15 Africánes in Fig. 11.

The annual frequency of Africánes per grid point (Fig. 3) is similar to a number of studies done elsewhere on tropical easterly lows using re-analysis data. Hurley and Boos (2015) found that the number of monsoon lows which occur in Australia vary between 1 and 6 per annum per grid point, with a similar frequency in India. They also identified the largest number of easterly waves over the western part of north Africa, where 6-8 lows occur per grid point per annum. This is on par with the number of Africánes identified over the Caprivi area (Fig. 3). Howard et al. (2019) identified between 1 and 1.4 Angola lows during January and February months per grid point over south-eastern Angola. In the presented research the number of Africánes in the Caprivi area is in a similar range but slightly higher with as many as 2.3 occurrences in the Caprivi area in January months.

The major focus of this paper is tropical lows which develop over the continent of Africa. The question arises to what extent landfalling tropical cyclones influence the high number of Africánes over eastern SA. Therefore, all westward moving tropical cyclones or storms which made landfall anywhere south of 15˚S over SA were identified by examining the data available from BOM Southern

Hemisphere Tropical Cyclone Portal[1], International Best Track Archive for Climate Stewardship (IBTrACS)[2] and RSMC La Reunion Archives[3]. The three data sources generally agree in the number, position and depth of tropical storms but their availability period differ. If a tropical cyclone was identified within a 300 km radius from an Africáne it was considered to have developed from a tropical cyclone (ex-tropical cyclone Africáne). The Africánes were then tracked throughout their entire life cycle as they moved westward over SA but still fulfilling the Africáne criteria as discussed in section 2. These Africánes were retained in the database as their characteristics closely mimic those of Africánes developing overland; especially as they penetrate into the central and western parts of the sub-continent.

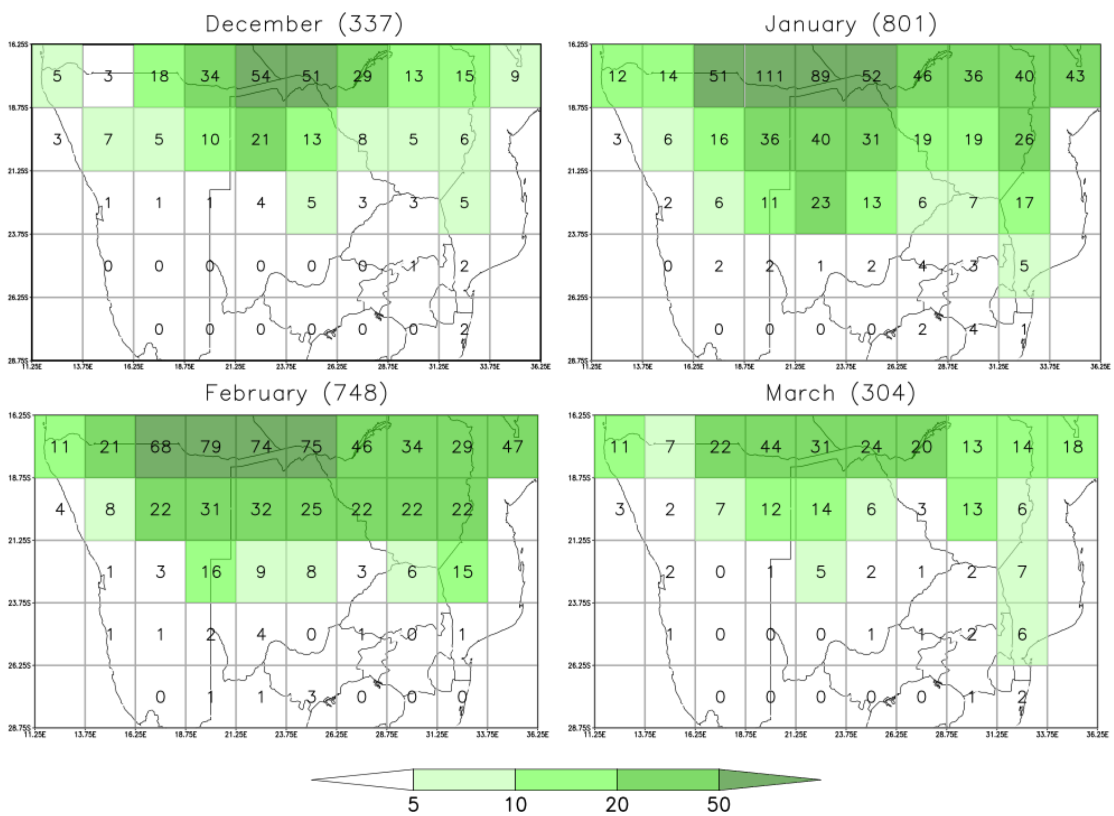

Figure 4: The number of Africánes per 2.5˚ x 2.5˚ NCEP grid box per month for the 39 summer seasons between 1981 and 2020. The total number of Africánes was calculated at 6-hourly time steps and more than one Africáne may be identified on a day. The total number of Africánes per month is indicated in brackets at the top of each graph.

[1] http://www.bom.gov.au/cyclone/tropical-cyclone-knowledge-centre/history/tracks/
[2] https://climatedataguide.ucar.edu/climate-data/ibtracs-tropical-cyclone-best-track-data
[3] http://www.meteo.fr/temps/domtom/La_Reunion/webcmrs9.0/anglais/index.html

Of the 2190 Africánes identified between 1981 and 2020, only 118 (± 5%) were associated with landfalling tropical cyclones or storms. In the eastern most grid points on Fig. 3, the percentage contribution of ex-tropical cyclones to Africánes varies between about 10% in the north, to 20% in the south. In January 1984 tropical cyclone Domoina made landfall over southern Mozambique and moved southwards into the borders of South Africa (Poolman and Terblanche, 1984). At 27.5˚S there are two grid points where at least 5 Africánes were identified (Fig. 3) per grid point. Three of the Africánes identified at these two grid points were ex-tropical cyclone Domoina which moved southward over South Africa.

A few of the ex-tropical cyclones stand out for their longevity and far westward reach over the sub-continent. Dineo made landfall over Mozambique on 15 February 2017 (Moses and Ramotonto, 2018) and was identified as an Africáne until 28 February 2017 over northern Namibia (17.5˚S, 15˚E). Tropical cyclone Eline invaded Mozambique on 22 February 2000 (Dyson and Van Heerden, 2001) and made its way steadily westward (Reason and Keibel, 2004) to be situated over western Namibia (25˚S, 15˚E) on 29 February 2000. During the entire study period only two Africánes were identified at this grid point, one of them being ex-tropical cyclone Eline.

Ex-tropical cyclones which penetrate so far west into the sub-continent are very rare, as Malherbe et al. (2012) described how they generally weaken rapidly as they move over land. Howard et al. (2019) state that most synoptic tropical lows propagate westwards across SA but also found that the majority of tropical lows develop and decay over Angola. Dyson and Van Heerden (2002) as well as Triegaardt et al. (1991) discuss the semi-stationary and slow-moving nature of these tropical lows while Webster (2019) shows an example of a tropical low moving eastwards over the sub-continent and into the Mozambique Channel.

5. Africáne circulation dynamics

This section provides a brief description of the general circulation and associated dynamics when Africánes occur over SA. Emphasis is placed on describing the favourable anomalous circulation and dynamics when this tropical cyclone-like low occurs over SA. Environments conducive to the development of tropical cyclones include that sea surface temperatures (SST) should be higher than 26 °C, values of wind shear should be a minimum and surface convergence and Coriolis force should be present (Asnani, 2005). The atmosphere should be convectively unstable and there should be enhanced near-surface vorticity values and sufficient mid-level moisture (Halperin et al., 2013). As many Africánes develop overland, the SST criteria is absent, but it is informative to investigate the other factors identified as favourable for the development of tropical cyclones.

The circulation fields are presented in two ways. In Figs. 5 and 6 the average circulation fields are presented for all days on which Africánes occurred (*average Africáne days*) and this is compared to the average fields for all days over December to March 1981 to 2020 (*average all days*). Secondly, system centered composite fields were constructed for all Africáne days (*composite Africáne days*) and this is also compared with the system centered composite for all days (*composite all days*). The composite fields for *Africáne days* and for *all the days* are the average fields calculated after shifting the position of the circulation fields so that the centre of the low is at the triangle in Figs 7 and 8

On *average Africáne days,* the 850 hPa circulation shows a low located over south-eastern Angola with a trough extending southwards into South Africa (Fig. 5). The Indian Ocean High is prominent south-east of the country (Fig. 5) and this corresponds to findings from (Malherbe et al., 2012) who found positive geopotential anomalies south-east of the country during wet years (rainfall associated with Africánes is discussed in Section 6). The *average all days* 500 hPa winds (wind barbs in Fig. 5) indicate the position of the continental sub-tropical high centered at around 22˚S, 17˚E at 500 hPa and the winds north of 22˚S is mostly easterly. However, during *average Africáne days*, the circulation is cyclonic over south-eastern Angola and the winds east of the low backs to north-westerly. The 500 hPa continental sub-tropical high also occurs further south and west over Namibia on *average Africáne* days compared to *average all days*.

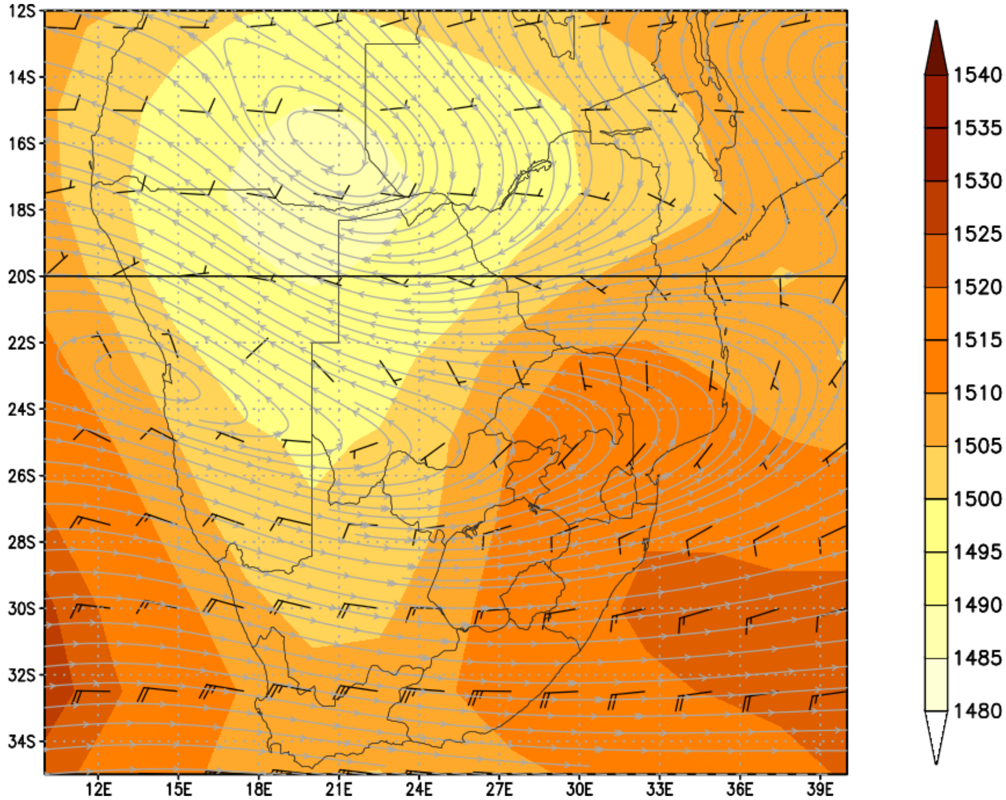

Figure 5: The 850 hPa geopotential heights (m; shaded) and 500 hPa winds on *average Africáne days* (streamlines) as well as the 500 hPa winds (knots; wind barbs) for *average all days* over the months December to March 1981-2020. The solid line at 20˚S depicts the area for the west-east cross section in Fig. 6.

The position of the Africáne at 850 hPa on *average Africáne days* is apparent in the negative (cyclonic) relative vorticity values close to 18˚E in the vertical cross section (Fig. 6). Negative vorticity values lie slightly eastward with height with the largest negative values occurring at around 700 hPa. This agrees with Howard et al. (2019) who used the average 600-800 hPa relative vorticity values to identify the tropical Angola low. The circulation remains cyclonic up to 400 hPa with positive relative vorticity values (not shown) only present between 300-400 hPa. This supports the first feature of the FTE (Section 2) that requires anomalously strong cyclonic circulation at 850 and 500 hPa and anticyclonic circulation at 300 hPa. The area of negative vorticity is closely linked to areas of wind convergence (Fig. 6). On average, wind convergence occurs up to nearly 400 hPa in an Africáne (see also Dyson and Van Heerden (2002)). Note the areas of wind divergence to the west of the Africáne through most of the troposphere. The winds on *average Africáne days* are from the east through most of the troposphere (Fig. 6). The cyclonic circulation associated with the Africáne is visible in the north-easterly winds east of the low and south-easterly winds west of the low. The anti-cyclonic circulation at 300 hPa cause the winds at this level to be westerly, although generally with wind strengths of 5 knots or less (see also Fig. 8B)

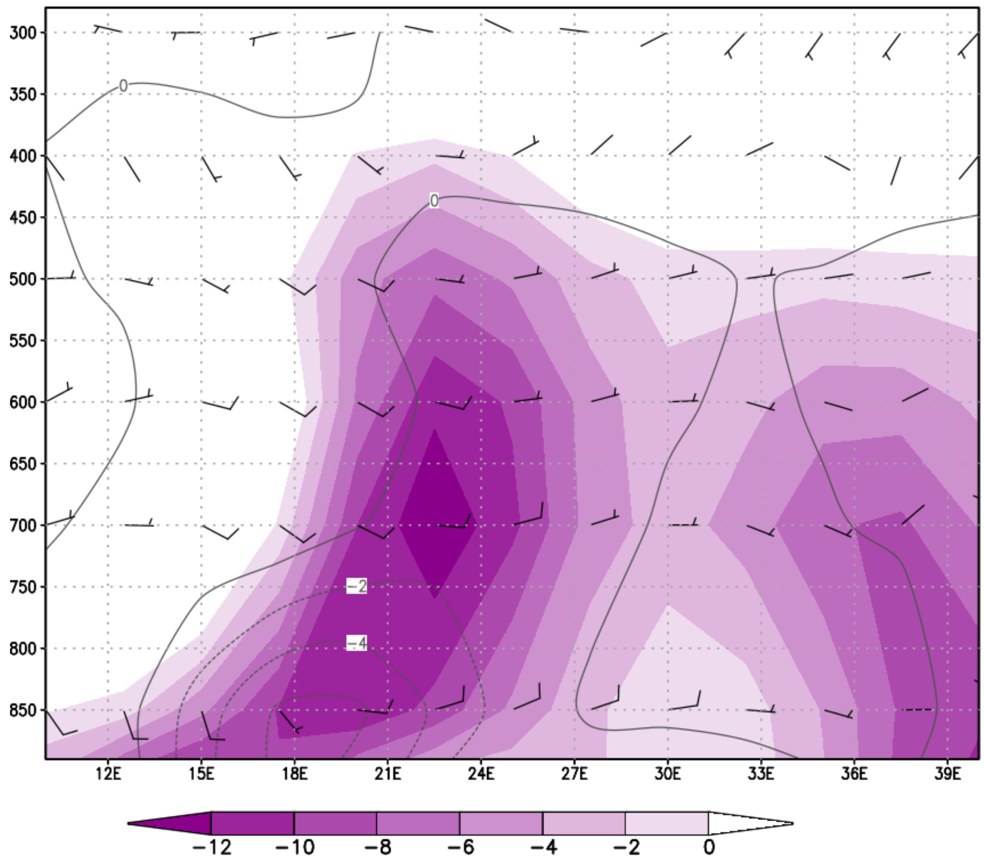

Figure 6. West-east cross section with height at 20˚S from 10˚ to 40˚E (see Fig. 5 for location). The shaded region is the relative vorticity (s^{-1}, values multiplied by 10^5), the contours are horizontal wind convergence (s^{-1}, values multiplied by 10^5) and the wind barbs are winds (knots) on *average Africáne days* over the months of December to March 1981-2020.

The 850 hPa specific humidity on *composite Africáne days* reach a maximum of 13 g kg^{-1} north-east of the Africáne (Fig. 7) and this is also the area with maximum 850 hPa wind convergence (-30 $*10^{-6}$ s^{-1}). The area to the east of the Africáne also experience wind divergence at 300 hPa. Considering Figs. 6 and 7, the area to the east of the Africáne is favorable for the development of convective rainfall. In section 6, it is shown how rainfall predominantly occurs on the eastern flank of the Africáne.

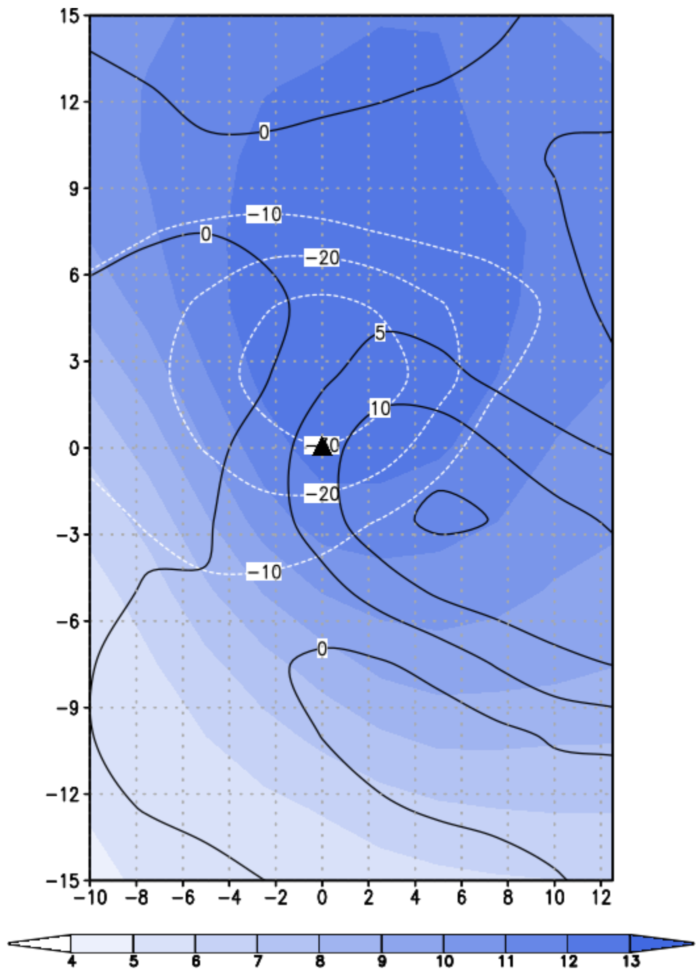

Figure 7: Composite of the 850 hPa specific humidity values (g kg^{-1}; shaded), 850 hPa horizontal wind convergence (s^{-1}, values multiplied by 10^5; white contours) and 300 hPa horizontal wind divergence (s^{-1}, values multiplied by 10^5; black contours) on *composite Africáne days* over the months December to March 1981-2020. The position of the Africáne is indicated by the triangle.

McBride and Zehr (1981) defined the Daily Genesis Potential (GP) as the difference in relative vorticity between 900 and 200 hPa. In the presented research we make a slight modification to the GP and by subtracting the 700 hPa relative vorticity from the 300 hPa relative vorticity. Large positive values indicate conditions favorable for tropical low development. Fig. 8a shows large positive values north-east of the Africáne on *composite Africáne days* and with anomalies of +10 s^{-1} when compared to *composite all day* GP value.

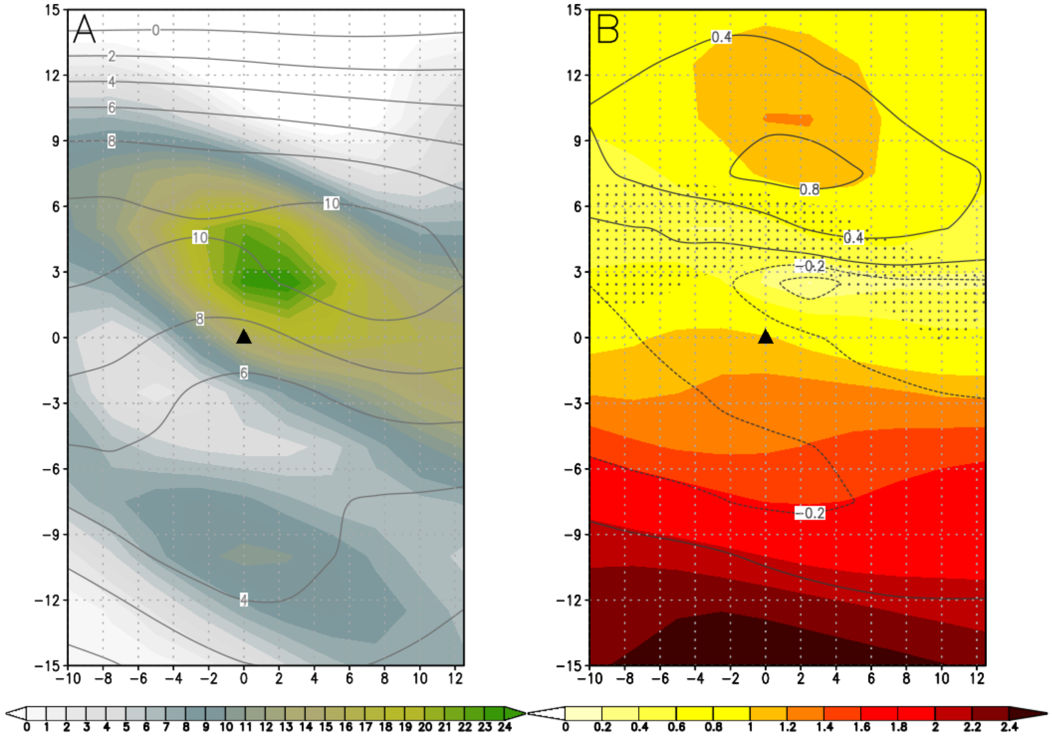

Figure 8: A. Composite of the Genesis Potential (GP) values on *composite Africáne days* (s^{-1}; shaded), and the anomaly between the GP values on *composite Africáne days* and *composite all days* over the months December to March 1981-2020 (contours). B. Average 700-400 hPa wind shear values (s^{-1}; colour shaded), 300 hPa wind speed < 5 knots (dotted shades) on *composite Africane days* and the anomaly between the 700-400 hPa wind shear values on *composite Africáne days* and *composite all days* over the months December to March 1981-2020 (contours). Positive anomaly values are above normal and the position of the Africáne is indicated by the triangle.

Wind shear values between 700 and 400 hPa on *composite Africáne days* reach values of very close to zero north of the Africáne (colour shades in Fig. 8b) in the approximate same location where 300 hPa wind speeds (dotted shades in Fig. 8b) is < 5 knots. The anomaly between *composite Africáne days* and *composite all days* (contours in Fig. 8b) shows that there is a decrease in wind shear in the vicinity of the Africáne with an increase in a band about 6˚N of the Africáne. This indicates the southward displacement of the area conducive to the development of tropical lows and corresponds to the southward shift of the mid-level subtropical high as discussed in Fig 5.

Fig. 5 illustrates the anomalous circulation over SA when Africánes occur and demonstrates the upright nature of the low. In Fig. 6 and 7 it is shown how ingredients to the area east and north-east of the Africáne combine to make conditions conducive to the development of convective precipitation. Figs. 7 and 8 show parameters in the vicinity of the Africáne to be similar to those favouring the development of tropical cyclones.

6. Contribution of Africánes to rainfall over southern Africa

The northern boundary of the study area where Africánes were identified in the NCEP data set is 17.5˚S. The contribution of rainfall on days when Africánes occurred (Africáne days) are considered for the area displayed in Fig. 9 which includes all of SA south of 15˚S. The proportion of rainfall on Africáne days are calculated over the entire domain for every Africáne day, regardless of the position of the low. We do not postulate that all rainfall which occurred over the domain on Africáne days is contributed to Africánes alone, but we endeavour to investigate how Africánes interact with other weather systems such as TTTs or the continental mid-tropospheric subtropical high to explain the rainfall distribution over the southern sub-continent of Africa.

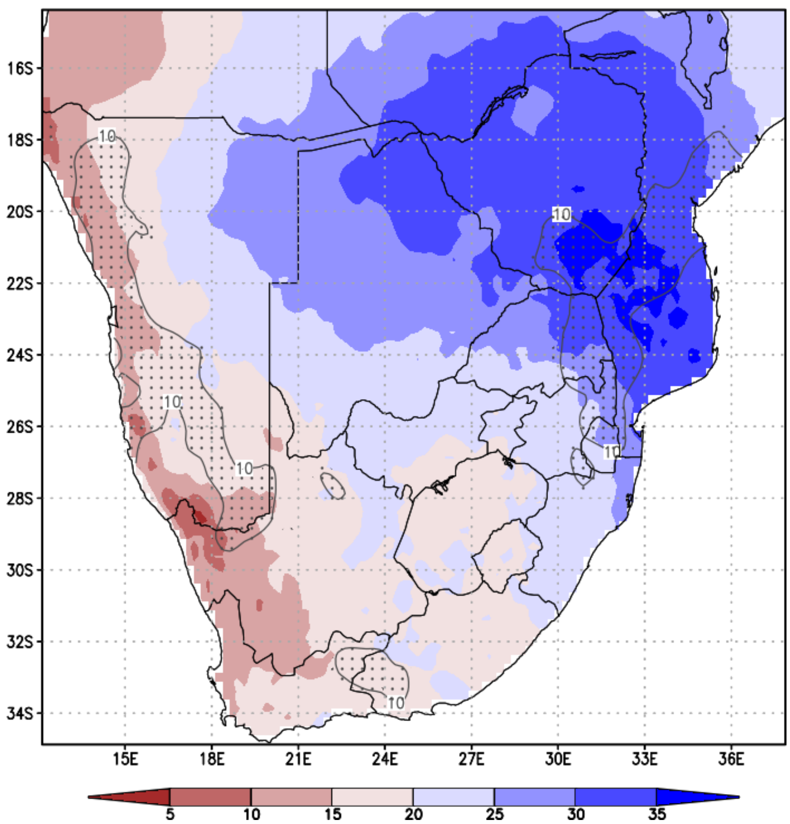

Figure 9: Composite of the proportion (%) of rainfall attributed to Africáne days as compared to the total December to March rainfall. The dotted shades indicate where the proportion (%) of the rainfall on ex-tropical cyclone Africáne days is more than 10% of the total rainfall on Africáne days.

Africánes were identified to occur on 879 days which is close to 19% of all the days during the study period. The percentage contribution of rainfall on Africáne days are compared to the total December through March rainfall (Fig. 9). Blue shades on Fig. 9 indicate a percentage contribution of more than

20%. Large areas of eastern Namibia, the entire Botswana, Zimbabwe and Mozambique and most of eastern South Africa receive more than 20% of their rainfall on days when Africánes occur. Percentages are as high as 30% over eastern Botswana and further eastwards over Zimbabwe and Mozambique. Africánes contribute significantly to rainfall over SA. On the Mozambique, South Africa, Zimbabwe border (MOZ/RSA/ZIM indicated on Fig. 1), the percentage contribution of Africáne rain to total Dec-Mar rainfall is as high as 35%. The high rainfall contribution in this area corresponds to the eastern peak in the frequency of Africánes around 32.5˚E (Fig. 3). The proximity to the warm, moist tropical air over the Mozambique Channel partly explains the higher percentage contribution to rainfall in this area as opposed to the Caprivi area where the moisture from the east and ITCZ would have been diluted due to the distance from the moisture source (Taljaard, 1996). Howard et al. (2019) attributed between 30-70% of rainfall in the area between 16-22˚S to tropical lows. In their study the highest proportion of rainfall occurs over southern Angola which is absent in the research presented in this paper. They also indicate a second peak in the contribution of total rainfall over eastern Zimbabwe and Mozambique where Fig. 9 shows that Africánes contribute the highest proportion to total rainfall. The reason for the differences in rainfall distribution is most likely due to Africánes only being investigated south of 17.5 ˚S and that lows over Angola were not considered. Furthermore (Howard et al., 2019) investigated only a 5-degree radius surrounding the centre of the low, while Africáne rain was calculated over the entire domain in Fig. 9 for all Africáne days, irrespective of position of the low.

About 12% of all December days were identified as Africáne days, and over most of the study area these days contribute less than 15% of December rain (Fig. 10). The rainfall contribution on Africáne days will henceforth be referred to as Africáne rain. Over the Caprivi area, Zimbabwe and central Mozambique, Africánes contribute up to 20% of total December rainfall. In January, the contribution of Africáne rain is more than 30% in the north and north-east of the study area including the northern and eastern extremes of South Africa. Over parts of Mozambique, Zimbabwe and eastern Botswana the contribution of Africáne rain is more than 40%. In February it is only the western extremes of the sub-continent that receives less than 30% of the total February rainfall on Africáne days. This is the month when Africáne rain contributes the most to the total monthly rainfall. Most of Botswana and Zimbabwe receive 40% of February rainfall on Africáne days. This value increases to 50% over the MOZ/RSA/ZIM area. Over South Africa, large areas receive more than 30% of the February rainfall on Africáne days, even as far south as the Eastern Cape province. From Fig. 4, February is also the month when Africánes occur the furthest south, explaining the rainfall contribution of Africánes to the total February rainfall over the southern areas in South Africa. By March, the contribution of Africáne rainfall to the total rainfall reduces to less than 25% over most of the study area, except for parts of Mozambique and Zimbabwe where the contribution remains more than 30%.

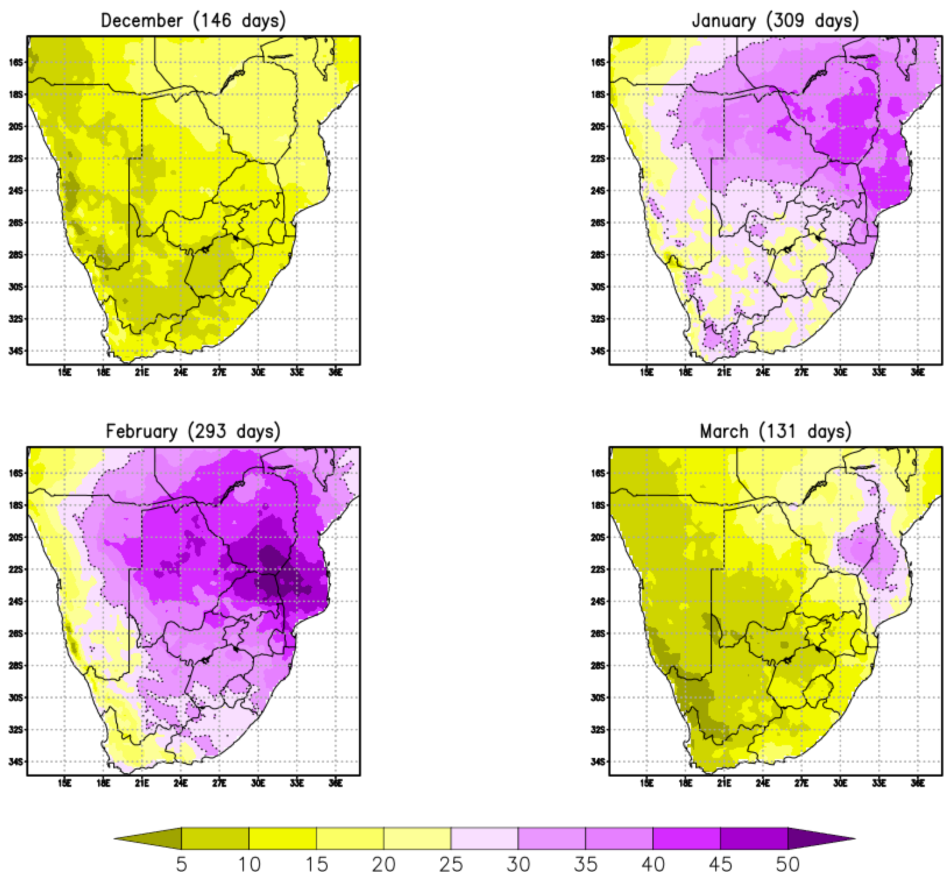

Figure 10: Composite of the proportion of monthly rainfall attributed to Africáne days. The number of Africáne days per month is indicated in brackets at the top of each graph. The 30 percentile is indicated by the dashed contour.

Over the western parts of Namibia and South Africa, less than 10% of the total Dec-Mar rainfall occurs on Africáne days (Fig. 9). These areas are arid and less than 50 mm rainfall occurs annually and even less over the coastal Namib desert (Suhling et al., 2009). Namibia predominantly receives rainfall from October to April (Lu et al., 2016), but over south-western Namibia and the adjacent areas in South Africa, rainfall occurs in winter (Schulze, 2001, Taljaard, 1996). Rainfall over these areas is rare during Dec-Mar, the months under investigation in this paper. Even though the seasonal rainfall contribution on Africáne days over these areas is small, it is noteworthy that in January and February months between 25-35% of the monthly rainfall are contributed to Africáne days (Fig. 10).

The proportion of the rainfall on ex-tropical cyclones days to total Africáne rainfall are depicted with the dotted shades in Fig. 9. There were only 51 ex-tropical cyclone Africáne days during this study period, this is about 6% of all Africáne days. The contribution of rainfall of ex-tropical cyclones is less than 10% to Africáne rain over most of the study area. The exceptions being in the eastern extremes of the study area as well as the far western parts (Fig. 9). The eastern dotted area of 10% covers the MOZ/RSA/ZIM area and where the topography starts to increase rapidly to the eastern escarpment (Fig. 1). As tropical cyclones invade the sub-continent and weaken, the onshore flow they induce from the Mozambique Channel encounters the escarpment causing additional uplift and heavy rainfall (see for example Dyson and Van Heerden, 2001). It was noted in section 4 that ex-tropical cyclone Domoina was located over KwaZulu-Natal in January 1984. The highest 24 hr rainfall measured at a South African Weather Service rainfall station was on 31 January 1984 when 597 mm was measured at St Lucia (see Fig.1 for location) on the north coast of KwaZulu-Natal (Kruger, 2007). Despite this extreme rainfall event, less than 10% of the total Africáne rainfall can be contributed to ex-tropical cyclones over northern KwaZulu-Natal (Fig. 9). Malherbe et al. (2011) found that landfalling tropical systems from the Mozambique Channel contribute less than 10% of the annual rainfall over the eastern interior of SA but that they do contribute significantly to local widespread heavy rainfall events.

The 10% rainfall contribution of ex-tropical cyclone Africánes to the Africáne rainfall over Namibia is noteworthy (Fig. 9). The annual rainfall in this area varies between less than 50 mm along the coast to about 150 mm over the adjacent interior (Suhling et al., 2009). Africánes contribute less than 20% to the total Dec-Mar rainfall in the area but at least 10% of this can be contributed to ex-tropical cyclones which would have travelled across most of the sub-continent to influence the rainfall this far west. The 10% area shows a north-west south-east orientation extending to the 10% area over the Western Cape/Eastern Cape border in South Africa. The orientation of this area is most likely associated with TTTs which act as large corridors through which tropical air flows to the temperate latitudes. Reason and Keibel (2004) explain such a configuration of weather systems, when ex-tropical cyclone Eline moved all the way to western South Africa and then combined with a westerly trough to form a TTT.

The geographical distribution of Africáne rainfall at 15 selected locations are depicted in Fig. 11. The geographical position (referred to as location) of Africánes is indicated above the panel and the numbers in the top left corner correspond to those indicated in the top left corner of the selected grid boxes on Fig. 3. The rainfall is expressed as a percentage of the long term mean rainfall and values less than 100% are indicated in grey. Above normal rainfall mostly occurs east of the Africáne with rapid decline in rainfall to the west (Fig. 11). Location 1 is situated far west over northern Namibia and Africánes in this position are important for rainfall over Namibia as above normal rainfall occurs over most of this country. There is also a band of above normal rainfall stretching southward over South Africa and this could indicate the presence of TTTs, although the average 500 hPa geopotential heights do not indicate the presence of a westerly trough, it rather indicates the absence of a high pressure over the central parts of the sub-continent. Location 2 was identified as the grid point with the highest number of Africánes (Fig. 3). Above normal rainfall with the Africáne at location 2, is mostly confined to countries north of South Africa. The rainfall band stretching southwards is not as clear as for location 1 and the average 500 hPa geopotential heights show the presence of a high south of the Africáne which most likely prevents the southward transport of moisture. The relationship between the geopotential heights and rainfall distribution is quite clear. When the mid-tropospheric subtropical high pressure over SA is dominant, rainfall occurs in the north of the study area (i.e. locations 2, 4, 5, 8, 9, 12) while when the high is absent or a westerly trough occurs in association with the Africáne, rainfall tends to extend to the south (i.e. 1, 6, 10, 13, 15). Africánes situated over Zimbabwe and Mozambique (locations 8, 9 and 12) result in well above normal rainfall on the escarpment of South Africa, Zimbabwe and Mozambique and along the south coast of Mozambique. These grid points were identified as having a relatively large number of ex-tropical cyclones (Fig. 3) and at least 10% of all Africáne rain is attributed to ex-tropical cyclone Africánes in this area (Fig. 9). Only 5 Africánes were identified at location 15, two of which were ex-tropical cyclone Domoina, which caused very heavy rainfall over the coast of KwaZulu-Natal where the average Africáne rainfall is 1600% of the norm. The depth the of the low at location 15 is the lowest of all the lows (5840 m). The other lows all have central depths of between 5860 m and 5870 m, with the exception being location 11 where the depth is 5850 m. The Africánes identified at 22.5˚ S (locations 10 and 11 on Fig. 11) are important for rainfall over South Africa, Botswana and eastern Namibia, as widespread and heavy rainfall occur over large parts of these countries. Africánes do not occur this far south over the central interior regularly (28 to 41 events in 39 years Fig. 3) but when they do occur, they contribute significantly to rainfall. Due to the small number of Africánes at locations 13 (5), 14 (6) and 15 (5) on Fig. 11, the rainfall at these locations cannot be truly demonstrative, other than showing that widespread and very heavy rainfall occurs to the east of an Africáne when it exists south of 25˚S.

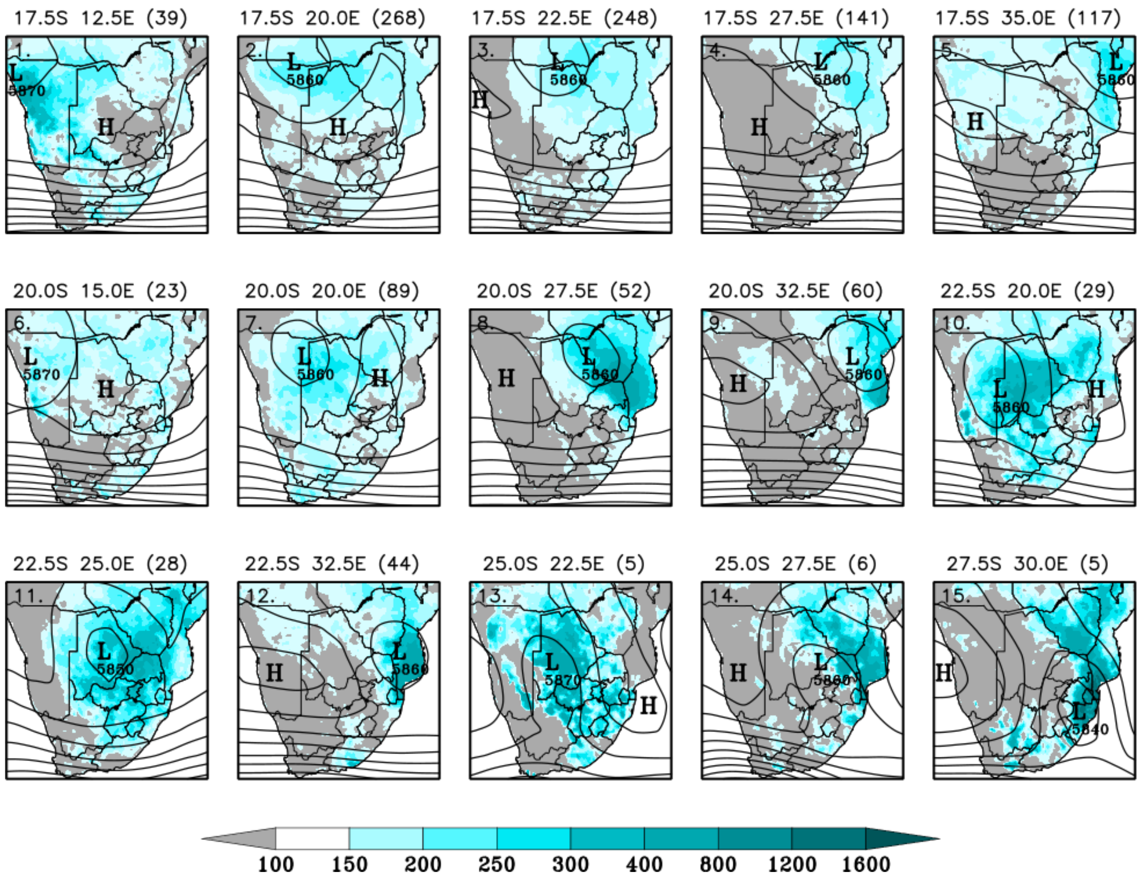

Figure 11. The average 500 hPa geopotential heights for all Africánes identified at 15 locations over southern Africa (contours). The geopotential value of each low is indicated on the graphs. Blue shades show the geographical distribution of the percentage of the normal daily rainfall (> 100%) attributed to Africánes at each of the 15 locations. Africáne rainfall percentage of less than 100% is indicated in grey. The location of the grid point at which the Africáne is located is indicated above each graph and the number of Africánes used to calculate the average Africáne rainfall and 500 hPa geopotential height at each location is indicated in brackets. The location number is indicated in the top left corner of each graph and corresponds to the numbers in the top left corner of Fig. 3.

The rainfall in a 7-degree radius surrounding each Africáne was used to create a composite map of average daily Africáne rainfall (Fig 12). The rainfall has been shifted so that the centre of the low is at the triangle in Fig. 12. The general distribution of the rainfall surrounding the Africáne is higher in the east and lower in the west. The highest rainfall occurs directly east of the Africáne with up to 13 mm per day and less than 6 mm per day west of the Africáne, decreasing with increasing distance to the west of the Africáne location. There is also a general tendency of higher rainfall amounts to occur slightly north-west of the Africáne stretching to the south-east (see the 5 mm isohyet on Fig. 12). This orientation represents the cloud bands associated with TTTs (Hart et al., 2010). Howard et al. (2019), Reason and Jagadheesha (2005) and other authors also found that anomalously high rainfall occurs east of a strong Angola low. In regions where tropical lows have an almost exclusively westward movement such as AELs over northern Africa (Gu et al., 2004) and monsoon lows in Australia (Berry et al., 2012) the anomalous rainfall occur to the west of the low.

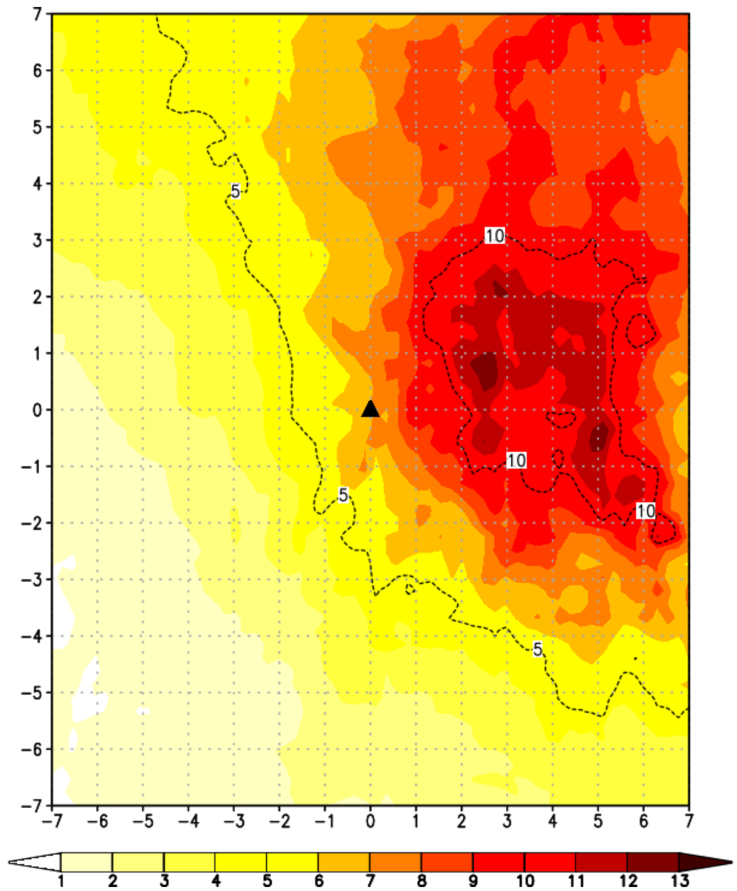

Figure 12: A composite of daily rainfall for all Africáne days centred around the centroid of the Africáne (mm/day). The triangle shows the location of the Africáne and the 5 and 10 mm contours are indicated by dotted lines

7. Interannual variability

The time series of the total number of Africánes per season is shown by the dashed line in Fig. 13. The average number of Africánes per season is 56 and the standard deviation is 31, indicating the high variability in the time series. There were as few as 4 Africánes in 1985/1986 and as many as 147 in 1999/2000.

The total number of Africánes per late summer were standardised with respect to the long-term average and standard deviation. These are shown in the bar graphs in Fig. 13 as the standardised index of Africánes. At the start of the study period (1981/1982 to 1986/1987) there were 6 consecutive seasons when the number of Africánes were below normal, while an above normal number of Africánes occurred for 5 successive years in the late 1990s (1995/1996 to 1999/2000). There were 13 seasons when the index of Africánes were higher than 0.5 (substantially above normal) and 14 when it was less than -0.5 (substantially below normal).

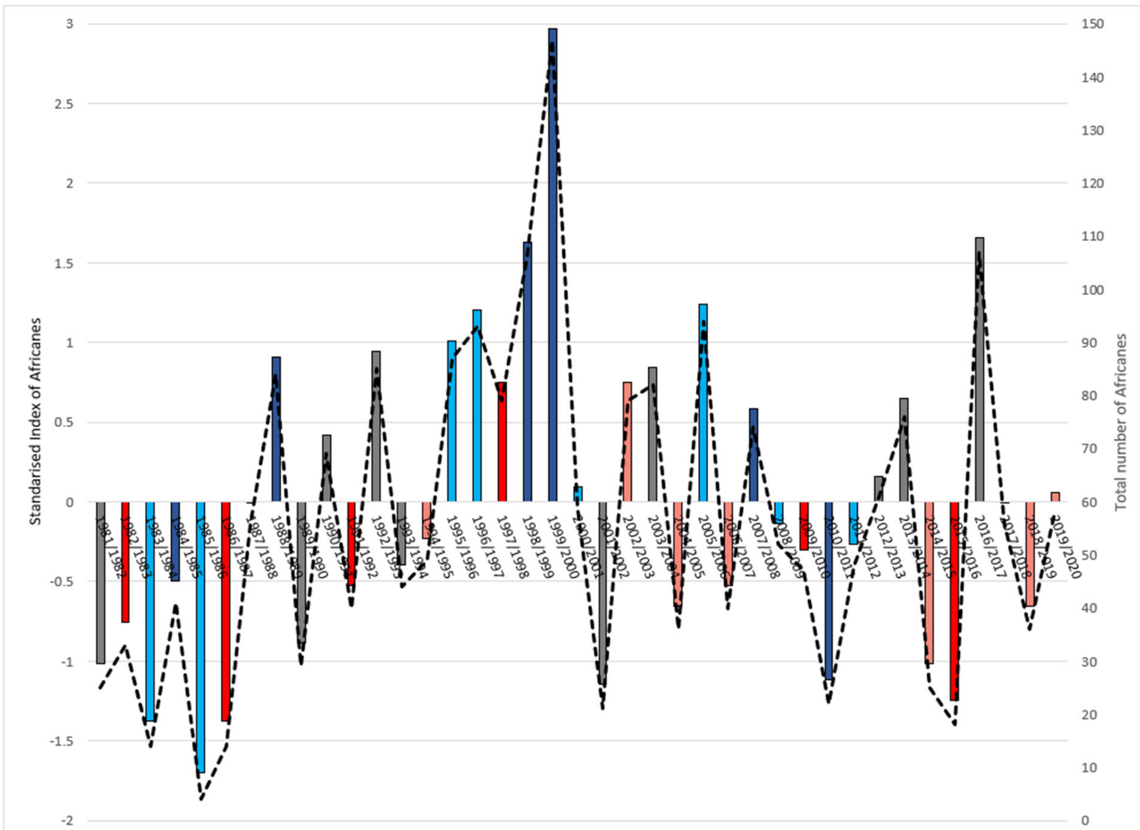

Figure 13: Standardized index of Africánes for late summers from 1981/1982 to 2019/2020 (bars). The dashed line indicates the total number of Africánes per summer season (Dec-Mar). The dark blue (red) bars indicate the seasons when the December January February (DJF) Oceanic Niño Index (ONI) was less than -1 (more than 1). Light blue (red) bars indicate those seasons when the ONI was less than -0.5 (more than 0.5)

The average daily rainfall for days when Africánes occurred in the seasons when the index of Africánes were substantially above and below normal (see Fig. 13) was calculated and compared to the long-term daily rainfall (Fig. 14). There were 13 seasons (566 days) when the index of Africánes were substantially above normal and 15 seasons (244 days) when it was substantially below normal. The influence of a high frequency of Africánes on rainfall over the southern sub-continent of Africa is clearly seen in Fig. 14. In the seasons when substantially above normal Africánes occur, the daily

Africáne rainfall is remarkably higher than when below-normal Africánes occur. Most of SA receives more than 100% (white and green shades) of the long-term daily rainfall in seasons when substantially above normal Africánes occur. The percentage is as high as 200% in the MOZ/RSA/ZIM area. Of the 51 ex-tropical cyclone Africáne days, 28 occurred when there were substantially above normal Africánes and these systems contribute to the copious rainfall in the MOZ/RSA/ZIM area (Fig. 9). In seasons when below number of Africánes occur, the 100% percentile of the long-term daily rainfall is located much further east over SA. However, there is still substantial rainfall over Mozambique and Zimbabwe (Fig. 14). The higher proportion of Africáne rainfall in the east is most likely due to the 15 ex-tropical cyclone days when substantially below normal Africánes occur. The western parts of South Africa, Botswana and the entire Namibia receive below normal rainfall when the number of Africánes in a season is substantially below normal.

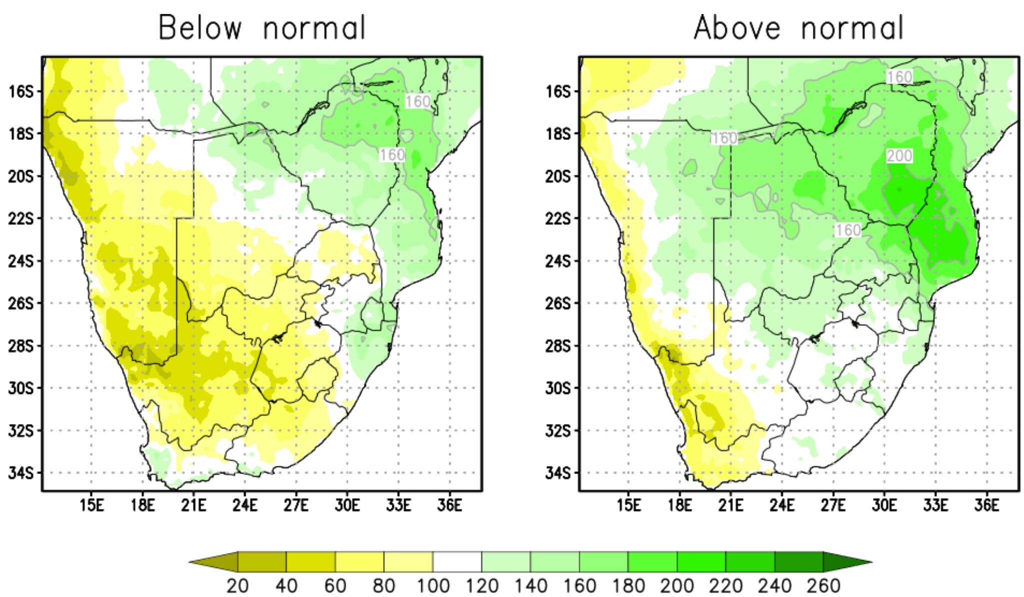

Figure 14: Composite of the proportion (%) of rainfall for Africáne days in the seasons when the index of Africánes was substantially below normal (index of Africánes < 0.5) (left) and above normal (index of Africánes >0.5) (right). The 160 and 200% contours are indicated in grey.

The interannual variability of Africánes is compared to ENSO in Fig. 13. The correlation between the index of Africánes and the Oceanic Niño Index (ONI) (available from https://origin.cpc.ncep.noaa.gov/products/analysis_monitoring/ensostuff/ONI_v5.php) for December January February (DJF) is -0.38 (significant up to the 5% confidence level). The frequency of Africánes were determined for all strong ENSO events (ONI ≤ -1 for La Niña and ONI ≥ 1 for El Niño) and are compared to the geographical distribution of all Africánes (Fig. 15). Fewer Africánes occur during strong El Niño events over most of the study area, the exception being northern

Namibia where slightly more Africánes were identified. Sea surface temperatures off the coast of northern Namibia/Angola have been found to be above normal during El Niño events (Florenchie et al., 2004) and it is possible that these warm Benguela Niños contribute to the above normal number of Africánes over northern Namibia during El Niño events. There is also slightly more Africánes during strong El Niño seasons at 25˚S, where the total number of Africánes vary between only 0.05 and 0.36 per annum. The largest differences between the average number of Africánes per grid point and the average number during strong El Niño events are over the Caprivi area and further eastwards where there are between 1 to 4 Africánes fewer per annum. The converse is true during La Niña events when there are 3 to 4 more Africánes in this area per season. In general, the annual frequency of Africánes is higher during strong La Niña events (Fig. 15). There are more Africánes than normal at all the grid boxes with the exception of central Botswana where fewer Africánes occur on average during strong La Niña years, although these anomalies are generally < 0.5.

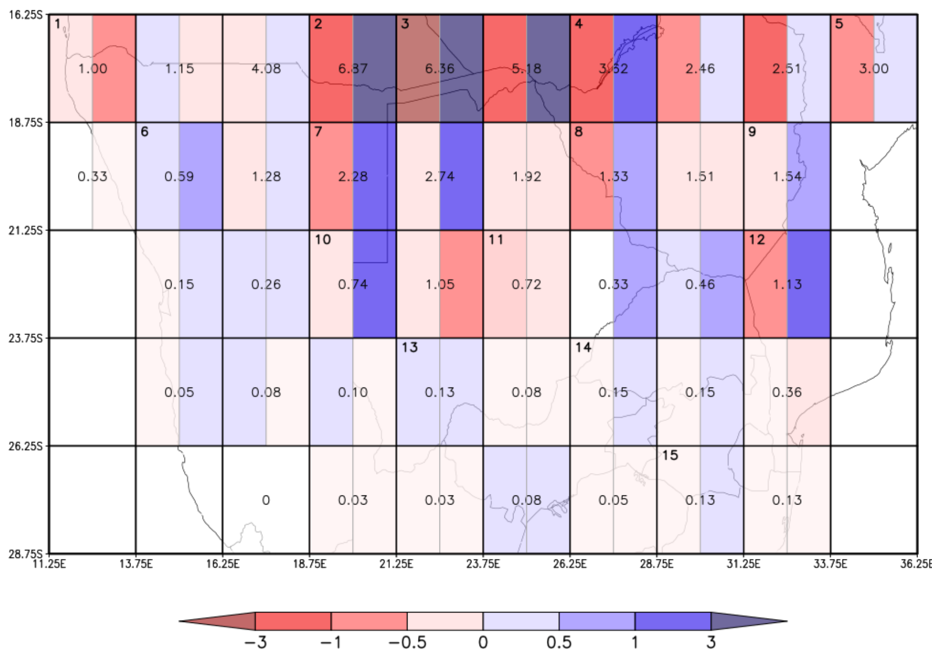

Figure 15: Annual anomalous Africáne frequency for strong El Niño and La Niña seasons for each NCEP grid box. Each grid box is divided in a left-hand box (El Niño) and a right-hand box (La Niña) and the shades indicate the deviation from the annual Africáne frequency (written in each grid box). The numbers in the top left-hand corner of each grid box corresponds to the 15 locations in figure 11. As example consider the grid box indicated by location number 2. The annual frequency of Africánes in this grid box is 6.87. During strong El Niño seasons there is between 1 and 3 fewer Africánes per annum in this grid box and during strong La Niña seasons there is > 3 Africánes more per season.

It is well established that La Niña years are associated with above normal rainfall over SA (see for example Jury (1996)). During these wet periods there are positive geopotential anomalies, throughout the troposphere, south-east and east of the sub-continent. This enhances the westward advection of moist tropical air into the sub-content and this in turn makes conditions conducive to the development of tropical disturbances (Malherbe et al., 2012). During El Niño events, rainfall over SA is generally below normal and during these dry periods, there is a cyclonic anomaly in the geopotential heights south-east of South Africa.

The average Africáne daily rainfall for all strong El Niño and La Niña seasons is compared to the long-term average daily rainfall in Fig. 16. The proportion of rainfall on Africáne days during strong La Niña seasons is above 100% over much of the northern parts of the study area. Over northern Limpopo province in South Africa, the contribution is as high as 200%, with the maximum contribution on the MOZ/RSA/ZIM area (> 240%). The average daily rainfall for Africáne days over Namibia and western South Africa is below normal, during strong La Niña events. The average daily rainfall on Africáne days during strong El Niño events is below normal over most of the study area. It is only over the far northern and eastern extremes of the study area where rainfall is still above normal on days when Africánes occur during strong El Niño events.

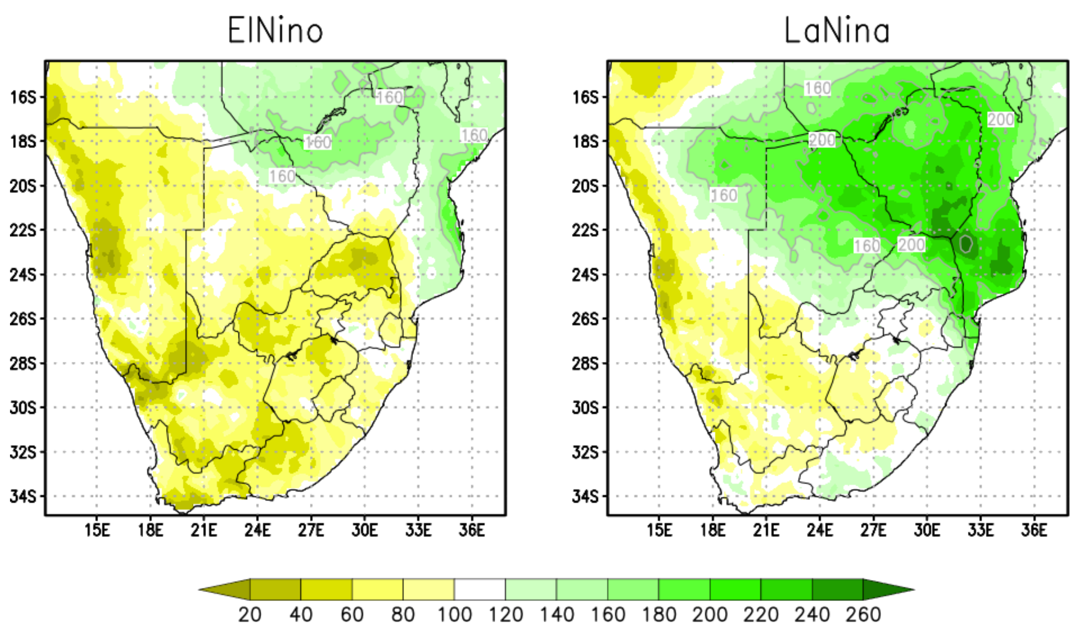

Figure 16: Composite of the proportion (%) of rainfall for all Africáne days when strong El Niño (left) and La Niña (right) seasons occurred. The 160 and 200% contours are indicated in grey.

The ONI for DJF was used to classify La Niña (ONI ≤ -0.5, light blue on Fig. 13) and strong La Niña seasons (ONI ≤ -1, dark blue on Fig. 13). The same was done for El Niño (ONI ≥ 0.5, light red on Fig.

13) and strong El Niño (ONI ≥ 1, dark red on Fig. 13). There were 13 La Niña seasons during the 39 seasons investigated, 7 of these (54%) were associated with substantially above normal Africánes and 4 (31%) with substantially below normal Africánes. When strong La Niña years occurred (there were 6), 4 (67%) were associated with substantially above normal Africánes. There were 14 El Niño seasons in the study period, 8 of them resulted in substantially below normal Africánes. Only 2 El Niño events were associated with substantially above normal Africánes namely the 1997/1998 season and the 2002/2003 season. Reason and Jagadheesha (2005) and Blamey et al. (2018) postulate that the drought of the 1997/1998 El Niño event was not as intense as predicted due to the presence of stronger Angola low during this season.

8. Discussion and conclusions

The presented research introduces the Africáne, a tropical cyclone-like low pressure system over the continent of SA. Strict circulation and thermodynamic criteria are applied to objectively identify Africánes which mostly develop over land, although about 6% of Africánes are the remanence of tropical cyclones which invade the sub-continent from the Mozambique Channel. Africánes are a very specific subset of Angola lows (Mulenga, 1998), strong Angola lows (Blamey et al., 2018, Howard and Washington, 2018) or tropical Angola lows (Howard et al., 2019).

Africánes are large, slow moving weather systems characterised by an upright low from the surface to the middle troposphere and displaced by a high near the tropopause (Dyson and Van Heerden, 2002). The low is cold cored near the surface but has a warm core in the middle and upper troposphere (Taljaard, 1985). Due to the slow-moving nature of the low, heavy rainfall may result over the same area for days on end, as transpired over the central interior of South Africa during February 1988, when heavy rainfall occurred for four consecutive days over the Free State province resulting in devastating floods (Triegaardt et al., 1991).

Africánes play an important role in the climate of southern sub-tropical Africa as they are responsible for widespread rainfall on their eastern flanks. Most Africánes occur in January but they extend further south in February months, when the proportion contribution of rainfall on Africáne days is more than 30% over SA with the exception of the west coast and adjacent interior. These far western parts of the study area are very dry with annual rainfall of less than 50 mm and Africánes contributing less than 15% to the total rainfall in the area. However, when Africánes are situated over north-western Namibia, well above normal rainfall occurs in Namibia.

There are two broad synoptic configurations associated with Africánes. Africánes sometimes combine with westerly troughs or TTTs which helps to pull the rain band southwards, causing significant rainfall over South Africa. Hart et al. (2010) describes three TTT events where they explain how the westerly trough combines with what they refer to as a strong Angola low. The tropical lows in the three events they describe were further classified as Africánes in the research presented here. Africánes play an important role in providing the tropical moisture, which is carried southward by the TTT, to cause rainfall further south. The second synoptic configuration associated with Africánes is when a well-developed mid-level subtropical high establishes itself south of the Africáne. The high prevents the rainfall from penetrating southward and rainfall is confined to the north of the study area.

A few Africánes develop from tropical cyclones moving in from the Mozambique Channel and these systems partly contribute to the high rainfall proportion contributed to Africánes over the escarpment of the MOZ/RSA/ZIM area. However, there are also Africánes which develop over the continent and move eastwards to eventually move into the Mozambique Channel (Webster, 2019). Africánes may then develop into tropical cyclones as they encounter the warm water in the Mozambique Channel as happened with tropical cyclone Idai in March 2019 (Yu et al., 2019). A similar process has been described to take place over north Africa, as the north Africa easterly low moves into the Atlantic Ocean and develop into Atlantic tropical cyclones (Burpee, 1972, Russell et al., 2017). In Australia, McBride and Keenan (1982) describe how tropical cyclones often develop over the northern coastline with forerunner systems forming overland.

The interannual variability of the number of Africánes per year is linked to ENSO. The correlation between the standardised index of Africánes and the ONI index is -0.38. Only 1 of 6 strong El Niño seasons resulted in substantially above normal number of Africánes and 2 of 6 strong La Niña seasons in below normal number of Africánes. The number of Africánes per season is closely related to the rainfall distribution over SA. Investigating the predictability of these systems could contribute to rainfall prediction on the short and medium time scales over SA.

9. Acknowledgements

The authors would like to thank the South African Water Research Commission who funded the research into continental tropical lows in southern Africa.

10. References

AMS. 2022. *Glossary of Meteorology* [Online]. [Accessed 13 April 2022].
ANTHES, R. 2016. *Tropical cyclones: their evolution, structure and effects*, Springer.
ASNANI, G. 2005. *Tropical meteorology*, Institute of Tropical Meteorology.
BERRY, G., THORNCROFT, C. & HEWSON, T. 2007. African easterly waves during 2004—Analysis using objective techniques. *Monthly weather review,* 135**,** 1251-1267.

BERRY, G. J., REEDER, M. J. & JAKOB, C. 2012. Coherent synoptic disturbances in the Australian monsoon. *Journal of Climate,* 25, 8409-8421.

BLAMEY, R., KOLUSU, S., MAHLALELA, P., TODD, M. & REASON, C. 2018. The role of regional circulation features in regulating El Niño climate impacts over southern Africa: A comparison of the 2015/2016 drought with previous events. *International Journal of Climatology,* 38, 4276-4295.

BURPEE, R. W. 1972. The origin and structure of easterly waves in the lower troposphere of North Africa. *Journal of Atmospheric Sciences,* 29, 77-90.

CAVICCHIA, L., VON STORCH, H. & GUALDI, S. 2014. A long-term climatology of medicanes. *Climate dynamics,* 43, 1183-1195.

CHIKOORE, H., VERMEULEN, J. H. & JURY, M. R. 2015. Tropical cyclones in the mozambique channel: January–March 2012. *Natural Hazards,* 77, 2081-2095.

CRIMP, S. 1997. *Mesoscale modelling of tropical-temperate troughs and associated systems over southern Africa*, Water Research Commission.

DYSON, L. & VAN HEERDEN, J. 2001. The heavy rainfall and floods over the northeastern interior of South Africa during February 2000. *South African Journal of Science,* 97, 80-86.

DYSON, L. & VAN HEERDEN, J. 2002. A model for the identification of tropical weather systems over South Africa. *Water SA,* 28, 249-258.

ENGELBRECHT, C. J., ENGELBRECHT, F. A. & DYSON, L. L. 2013. High-resolution model-projected changes in mid-tropospheric closed-lows and extreme rainfall events over southern Africa. *International Journal of Climatology,* 33, 173-187.

ENGELBRECHT, C. J., LANDMAN, W. A., ENGELBRECHT, F. A. & MALHERBE, J. 2015. A synoptic decomposition of rainfall over the Cape south coast of South Africa. *Climate Dynamics,* 44, 2589-2607.

FAVRE, A., HEWITSON, B., LENNARD, C., CEREZO-MOTA, R. & TADROSS, M. 2013. Cut-off lows in the South Africa region and their contribution to precipitation. *Climate dynamics,* 41, 2331-2351.

FLORENCHIE, P., REASON, C., LUTJEHARMS, J., ROUAULT, M., ROY, C. & MASSON, S. 2004. Evolution of interannual warm and cold events in the southeast Atlantic Ocean. *Journal of Climate,* 17, 2318-2334.

FUNK, C., PETERSON, P., LANDSFELD, M., PEDREROS, D., VERDIN, J., SHUKLA, S., HUSAK, G., ROWLAND, J., HARRISON, L. & HOELL, A. 2015. The climate hazards infrared precipitation with stations—a new environmental record for monitoring extremes. *Scientific data,* 2, 1-21.

GU, G., ADLER, R. F., HUFFMAN, G. J. & CURTIS, S. 2004. African easterly waves and their association with precipitation. *Journal of Geophysical Research: Atmospheres,* 109.

HALPERIN, D. J., FUELBERG, H. E., HART, R. E., COSSUTH, J. H., SURA, P. & PASCH, R. J. 2013. An evaluation of tropical cyclone genesis forecasts from global numerical models. *Weather and Forecasting,* 28, 1423-1445.

HARRISON, M. 1984. A generalized classification of South African summer rain-bearing synoptic systems. *Journal of Climatology,* 4, 547-560.

HART, N., REASON, C. & FAUCHEREAU, N. 2010. Tropical–extratropical interactions over southern Africa: Three cases of heavy summer season rainfall. *Monthly weather review,* 138, 2608-2623.

HART, N. C., REASON, C. J. & FAUCHEREAU, N. 2013. Cloud bands over southern Africa: seasonality, contribution to rainfall variability and modulation by the MJO. *Climate dynamics,* 41, 1199-1212.

HAUSER, S., GRAMS, C. M., REEDER, M. J., MCGREGOR, S., FINK, A. H. & QUINTING, J. F. 2020. A weather system perspective on winter–spring rainfall variability in southeastern Australia during El Niño. *Quarterly Journal of the Royal Meteorological Society,* 146, 2614-2633.

HODGES, K. I. 1994. A general method for tracking analysis and its application to meteorological data. *Monthly Weather Review,* 122, 2573-2586.

HOWARD, E. & WASHINGTON, R. 2018. Characterizing the synoptic expression of the Angola low. *Journal of Climate,* 31**,** 7147-7165.

HOWARD, E., WASHINGTON, R. & HODGES, K. I. 2019. Tropical lows in southern Africa: Tracks, rainfall contributions, and the role of ENSO. *Journal of Geophysical Research: Atmospheres,* 124**,** 11009-11032.

HUNT, K. M. & FLETCHER, J. K. 2019. The relationship between Indian monsoon rainfall and low-pressure systems. *Climate Dynamics,* 53**,** 1859-1871.

HUNT, K. M., TURNER, A. G., INNESS, P. M., PARKER, D. E. & LEVINE, R. C. 2016. On the structure and dynamics of Indian monsoon depressions. *Monthly Weather Review,* 144**,** 3391-3416.

HURLEY, J. V. & BOOS, W. R. 2015. A global climatology of monsoon low-pressure systems. *Quarterly Journal of the Royal Meteorological Society,* 141**,** 1049-1064.

JURY, M. R. 1996. Regional teleconnection patterns associated with summer rainfall over South Africa, Namibia and Zimbabwe. *International Journal of Climatology: A Journal of the Royal Meteorological Society,* 16**,** 135-153.

KRUGER, A. 2007. Climate of South Africa. Precipitation.: South African Weather Service.

LAING, A. & EVANS, J. 2016. *Introduction to Tropical Meteorology. 2nd Edition. A comprehensive Online and Print Textbook. Version 4.0.* [Online]. Available: https://www.meted.ucar.edu/tropical/textbook_2nd_edition/ [Accessed].

LU, X., WANG, L., PAN, M., KASEKE, K. F. & LI, B. 2016. A multi-scale analysis of Namibian rainfall over the recent decade–comparing TMPA satellite estimates and ground observations. *Journal of Hydrology: Regional Studies,* 8**,** 59-68.

MALHERBE, J., ENGELBRECHT, F. A., LANDMAN, W. A. & ENGELBRECHT, C. J. 2012. Tropical systems from the southwest Indian Ocean making landfall over the Limpopo River Basin, southern Africa: a historical perspective. *International Journal of Climatology,* 32**,** 1018-1032.

MAY, P. T., MATHER, J. H., VAUGHAN, G., JAKOB, C., MCFARQUHAR, G. M., BOWER, K. N. & MACE, G. G. 2008. The tropical warm pool international cloud experiment. *Bulletin of the American Meteorological Society,* 89**,** 629-646.

MCBRIDE, J. & KEENAN, T. 1982. Climatology of tropical cyclone genesis in the Australian region. *Journal of Climatology,* 2**,** 13-33.

MCBRIDE, J. L. & ZEHR, R. 1981. Observational analysis of tropical cyclone formation. Part II: Comparison of non-developing versus developing systems. *Journal of Atmospheric Sciences,* 38**,** 1132-1151.

MOSES, O. & RAMOTONTO, S. 2018. Assessing forecasting models on prediction of the tropical cyclone Dineo and the associated rainfall over Botswana. *Weather and climate extremes,* 21**,** 102-109.

MULENGA, H. 1998. *Southern African climatic anomalies, summer rainfall and the Angola low.* Ph.D., University of Cape Town.

POOLMAN, E. & TERBLANCHE, D. 1984. Tropiese Siklone Domoina en Imboa. *South African Weather Bureau Newsletter. 420, pp. 37-45.* .

RAMAGE, C. S. 1995. Forecasters Guide to Tropical Meteorology. Updated. AIR WEATHER SERVICE SCOTT AFB IL.

REASON, C. & JAGADHEESHA, D. 2005. A model investigation of recent ENSO impacts over southern Africa. *Meteorology and Atmospheric Physics,* 89**,** 181-205.

REASON, C. & KEIBEL, A. 2004. Tropical cyclone Eline and its unusual penetration and impacts over the southern African mainland. *Weather and forecasting,* 19**,** 789-805.

REASON, C., LANDMAN, W. & TENNANT, W. 2006. Seasonal to decadal prediction of southern African climate and its links with variability of the Atlantic Ocean. *Bulletin of the American Meteorological Society,* 87**,** 941-956.

RICHARD, Y., FAUCHEREAU, N., POCCARD, I., ROUAULT, M. & TRZASKA, S. 2001. 20th century droughts in southern Africa: spatial and temporal variability, teleconnections with oceanic and atmospheric conditions. *International Journal of Climatology: A Journal of the Royal Meteorological Society,* 21, 873-885.

RIEHL, H. 1979. *Climate and Weather in the Tropics*, Academic Press.

RUSSELL, J. O., AIYYER, A., WHITE, J. D. & HANNAH, W. 2017. Revisiting the connection between African easterly waves and Atlantic tropical cyclogenesis. *Geophysical Research Letters,* 44, 587-595.

SCHULZE, R. 2001. *SOUTH AFRICAN ATLAS OF AGROHYDROLOGY AND CLIMATOLOGY* [Online]. Available: http://planet.uwc.ac.za/NISL/Invasives/Assignments/GARP/atlas/atlas.htm [Accessed 29 April 2019].

SEIDEL, D. J., ROSS, R. J., ANGELL, J. K. & REID, G. C. 2001. Climatological characteristics of the tropical tropopause as revealed by radiosondes. *Journal of Geophysical Research: Atmospheres,* 106, 7857-7878.

SINGLETON, A. & REASON, C. 2007. Variability in the characteristics of cut-off low pressure systems over subtropical southern Africa. *International Journal of Climatology: A Journal of the Royal Meteorological Society,* 27, 295-310.

SUHLING, F., MARTENS, A. & MARAIS, E. 2009. How to enter a desert—patterns of Odonata colonisation of arid Namibia. *International Journal of Odonatology,* 12, 287-308.

TALJAARD, J. 1953. The mean circulation in the lower troposphere over southern Africa. *South African Geographical Journal,* 35, 33-45.

TALJAARD, J. 1985. Cut-off Lows in the South African Region. *South African Weather Bureau Technical Paper.* South African Weather Bureau Technical Paper, 14.

TALJAARD, J. 1995. Atmospheric circulation systems, synoptic climatology and weather phenomena of South Africa. Part 2: Atmospheric circulation systems in the South African region. South African Weather Bureau Technical Paper No 28.

TALJAARD, J. 1996. Atmospheric circulation systems, synoptic climatology and weather phenomena of South Africa: Part 6 Rainfall in South Africa.: South African Weather Bureau Technical Paper No 32. .

TANG, S., SMITH, R. K., MONTGOMERY, M. T. & GU, M. 2016. Numerical study of the spin-up of a tropical low over land during the Australian monsoon. *Quarterly Journal of the Royal Meteorological Society,* 142, 2021-2032.

TRIEGAARDT, D., VAN HEERDEN, J. & STEYN, P. 1991. Anomalous precipitation and floods during February 1988.: South African Weather Service Technical Paper, 23.

TYSON, P. D. & PRESTON-WHYTE, R. A. 2000. *Weather and climate of southern Africa*, Oxford University Press.

VAN DEN HEEVER, S., D'ABRETON, P. & TYSON, P. 1997. Numerical simulation of tropical-temperate troughs over southern Africa using the CSU RAMS model. *South African journal of science,* 93, 359-365.

WASHINGTON, R. & TODD, M. 1999. Tropical–temperate links in southern African and Southwest Indian Ocean satellite-derived daily rainfall. *International Journal of Climatology: A Journal of the Royal Meteorological Society,* 19, 1601-1616.

WEBSTER, E. 2019. *A synoptic climatology of Continental Tropical Low pressure systems over southern Africa and their contribution to rainfall over South Africa.* M.Sc., University of Pretoria.

WILLIAMS, F., RENARD, R., JUNG, G., TOMKINS, R. & PICARD, R. 1984. Forecasters Handbook for the Southern African Continent and Atlantic/Indian Ocean Transit. NAVAL ENVIRONMENTAL PREDICTION RESEARCH FACILITY MONTEREY CA.

YU, P., JOHANNESSEN, J. A., YAN, X.-H., GENG, X., ZHONG, X. & ZHU, L. 2019. A Study of the Intensity of Tropical Cyclone Idai Using Dual-Polarization Sentinel-1 Data. *Remote Sensing,* 11, 2837.

ZUNCKEL, M., HONG, Y., BRASSEL, K. & O'BEIRNE, S. 1996. Characteristics of the nocturnal boundary layer: Okaukuejo, Namibia, during SAFARI-92. *Journal of Geophysical Research: Atmospheres,* 101, 23757-23766.

List of Figures

Figure 1: Topographical and location map of southern Africa. The dotted shades indicate the Caprivi area and the border between Mozambique, South Africa and Zimbabwe (MOZ/RSA/ZIM).

Figure 2: Flow diagram illustrating the procedure used to objectively identify Africánes over southern Africa.

Figure 3: Total number of Africánes per 2.5˚ x 2.5˚ NCEP grid box for the 39 summer seasons (Dec-Mar) between 1981 and 2020 and the annual Africáne frequency (number in brackets). The total number of Africánes was calculated at 6-hourly time steps and more than one Africáne may be identified on a day. The total number of Africánes are indicated in the centre of each grid box. The number at the bottom of the grid box indicates the number of ex-tropical cyclone Africánes identified in the grid box. The number in the top left of the grid box is the location number of 15 Africánes in Fig. 11.

Figure 4: The number of Africánes per 2.5˚ x 2.5˚ NCEP grid box per month for the 39 summer seasons between 1981 and 2020. The total number of Africánes was calculated at 6-hourly time steps and more than one Africáne may be identified on a day. The total number of Africánes per month is indicated in brackets at the top of each graph.

Figure 5: The 850 hPa geopotential heights (m; shaded) and 500 hPa winds on *average Africáne days* (streamlines) as well as the 500 hPa winds (knots; wind barbs) for *average all days* over the months December to March 1981-2020. The solid line at 20˚S depicts the area for the west-east cross section in Fig. 6.

Figure 6. West-east cross section with height at 20˚S from 10˚ to 40˚E (see Fig. 5 for location). The shaded region is the relative vorticity (s^{-1}, values multiplied by 10^5), the contours are horizontal wind convergence (s^{-1}, values multiplied by 10^5) and the wind barbs are winds (knots) on *average Africáne days* over the months of December to March 1981-2020.

Figure 7: Composite of the 850 hPa specific humidity values ($g\ kg^{-1}$; shaded), 850 hPa horizontal wind convergence (s^{-1}, values multiplied by 10^5; white contours) and 300 hPa horizontal wind divergence (s^{-1}, values multiplied by 10^5; black contours) on *composite Africáne days* over the months December to March 1981-2020. The position of the Africáne is indicated by the triangle.

Figure 8: A. Composite of the Genesis Potential (GP) values on *composite Africáne days* (s^{-1}; shaded), and the anomaly between the GP values on *composite Africáne days* and *composite all days* over the months December to March 1981-2020 (contours). B. Average 700-400 hPa wind shear values (s^{-1}; colour shaded), 300 hPa wind speed < 5 knots (dotted shades) on *composite Africane days* and the anomaly between the 700-400 hPa wind shear values on *composite Africáne days* and *composite all days* over the months December to March 1981-2020 (contours). Positive anomaly values are above normal and the position of the Africáne is indicated by the triangle.

Figure 9: Composite of the proportion (%) of rainfall attributed to Africáne days as compared to the total December to March rainfall. The dotted shades indicate where the proportion (%) of the rainfall on ex-tropical cyclone Africáne days is more than 10% of the total rainfall on Africáne days.

Figure 10: Composite of the proportion of monthly rainfall attributed to Africáne days. The number of Africáne days per month is indicated in brackets at the top of each graph. The 30 percentile is indicated by the dashed contour.

Figure 11. The average 500 hPa geopotential heights for all Africánes identified at 15 locations over southern Africa (contours). The geopotential value of each low is indicated on the graphs. Blue shades show the geographical distribution of the percentage of the normal daily rainfall (> 100%) attributed to Africánes at each of the 15 locations. Africáne rainfall percentage of less than 100% is indicated in grey. The location of the grid point at which the Africáne is located is indicated above each graph and the number of Africánes used to calculate the average Africáne rainfall and 500 hPa geopotential height at each location is indicated in brackets. The location number is indicated in the top left corner of each graph and corresponds to the numbers in the top left corner of Fig. 3.

Figure 12: A composite of daily rainfall for all Africáne days centred around the centroid of the Africáne (mm/day). The triangle shows the location of the Africáne and the 5 and 10 mm contours are indicated by dotted lines

Figure 13: Standardized index of Africánes for late summers from 1981/1982 to 2019/2020 (bars). The dashed line indicates the total number of Africánes per summer season (Dec-Mar). The dark blue (red) bars indicate the seasons when the December January February (DJF) Oceanic Niño Index (ONI) was less than -1 (more than 1). Light blue (red) bars indicate those seasons when the ONI was less than -0.5 (more than 0.5)

Figure 14: Composite of the proportion (%) of rainfall for Africáne days in the seasons when the index of Africánes was substantially below normal (index of Africánes < 0.5) (left) and above normal (index of Africánes >0.5) (right). The 160 and 200% contours are indicated in grey.

Figure 15: Annual anomalous Africáne frequency for strong El Niño and La Niña seasons for each NCEP grid box. Each grid box is divided in a left-hand box (El Niño) and a right-hand box (La Niña) and the shades indicate the deviation from the annual Africáne frequency (written in each grid box). The numbers in the top left-hand corner of each grid box corresponds to the 15 locations in figure 11. As example consider the grid box indicated by location number 2. The annual frequency of Africánes in this grid box is 6.87. During strong El Niño seasons there is between 1 and 3 fewer Africánes per annum in this grid box and during strong La Niña seasons there is > 3 Africánes more per season.

Figure 16: Composite of the proportion (%) of rainfall for all Africáne days when strong El Niño (left) and La Niña (right) seasons occurred. The 160 and 200% contours are indicated in grey.